

Global dynamics of healthy and cancer cells competing in the hematopoietic system

Wienecke Andersen, Morten; Hasselbalch, Hans; Kjær, Lasse; Skov, Vibe; Ottesen, Johnny T.

Published in:
Mathematical Biosciences

DOI:
[10.1016/j.mbs.2020.108372](https://doi.org/10.1016/j.mbs.2020.108372)

Publication date:
2020

Document Version
Peer reviewed version

Citation for published version (APA):
Wienecke Andersen, M., Hasselbalch, H., Kjær, L., Skov, V., & Ottesen, J. T. (2020). Global dynamics of healthy and cancer cells competing in the hematopoietic system. *Mathematical Biosciences*, 326(326), Article 108372. <https://doi.org/10.1016/j.mbs.2020.108372>

General rights

Copyright and moral rights for the publications made accessible in the public portal are retained by the authors and/or other copyright owners and it is a condition of accessing publications that users recognise and abide by the legal requirements associated with these rights.

- Users may download and print one copy of any publication from the public portal for the purpose of private study or research.
- You may not further distribute the material or use it for any profit-making activity or commercial gain.
- You may freely distribute the URL identifying the publication in the public portal.

Take down policy

If you believe that this document breaches copyright please contact rucforsk@kb.dk providing details, and we will remove access to the work immediately and investigate your claim.

Global dynamics of healthy and cancer cells competing in the hematopoietic system

May 8, 2020

Morten Andersen, Hans C. Hasselbalch, Lasse Kjær, Vibe Skov, Johnny T. Ottesen

Abstract

1 Stem cells in the bone marrow differentiate to ultimately become mature, functioning
2 blood cells through a tightly regulated process (hematopoiesis) including a stem cell niche
3 interaction and feedback through the immune system. Mutations in a hematopoietic stem
4 cell can create a cancer stem cell leading to a less controlled production of malfunctioning
5 cells in the hematopoietic system. This was mathematically modelled by Andersen et al.
6 (PLoS ONE, 12 (2017), pp. 1-18) including the dynamic variables: healthy and cancer
7 stem cells and mature cells, dead cells and an immune system response. Here, we apply a
8 quasi steady state approximation to this model to construct a two dimensional model with
9 four algebraic equations denoted the simple canctis model. The two dynamic variables are
10 the clinically available quantities *JAK2V617F* allele burden and the number of white blood
11 cells. The simple canctis model represents the original model very well. Complete phase
12 space analysis of the simple canctis model is performed, including proving the existence and
13 location of globally attracting steady states. Hence, parameter values from compartments
14 of stem cells, mature cells and immune cells are directly linked to disease and treatment
15 prognosis, showing the crucial importance of early intervention. The simple canctis model
16 allows for a complete analysis of the long term evolution of trajectories. In particular,
17 the value of the self renewal of the hematopoietic stem cells divided by the self renewal of
18 the cancer stem cells is found to be an important diagnostic marker and perturbing this
19 parameter value at intervention allows the model to reproduce clinical data. Treatment
20 at low cancer cell numbers allows returning to healthy blood production while the same
21 intervention at a later disease stage can lead to eradication of healthy blood producing
22 cells.

23 Assuming the total number of white blood cells is constant in the early cancer phase
24 while the allele burden increases, a one dimensional model is suggested and explicitly solved,

25 including parameters from all original compartments. The solution explicitly shows that
26 exogenous inflammation promotes blood cancer when cancer stem cells reproduce more
27 efficiently than hematopoietic stem cells.

28 1 Introduction

29 Production of blood cells is denoted hematopoiesis. In the bone marrow reside the hematopoi-
30 etic stem cells (HSC) that differentiate through multiple cell divisions into mature cells
31 (MC) such as neutrophils, platelets, and red blood cells [40]. The number of human HSC
32 has been estimated to be of the order of $10^4 - 10^5$ each dividing every 25th to 50th week [6],
33 [38]. An order of magnitude of 10^{11} mature blood cells are produced daily [68], correspond-
34 ing to millions per second, equivalent to 10 kg per year [43]. Clearly, a tight regulation of
35 blood cell production is crucial and disturbances to this regulation may be severe.

36 Mathematical modelling has a prominent role in the study of hematopoiesis and its
37 disorders and may be addressed from various areas of applied mathematics such as ordinary
38 differential equations (ODE) [20, 66, 46, 45, 59], partial differential equations (PDE) [58,
39 39, 28], delay differential equations [43, 3] or stochastic models [13, 12, 67, 34]. Böttcher
40 et al. [5] investigate replicative capacity of progenitors and differentiated cells and use an
41 ODE-model to investigate the cellular aging based on data for telomere lengths and discuss
42 implications for chronic myeloid leukemia. This approach relies on a discrete age structure,
43 whereas for example Doumic et al. [14] consider a continuous age structure including stem
44 cell dynamics, naturally leading to a PDE-formulation. Ashcroft et al. [2] focus on stem
45 cell dynamics and use stochastic modelling to investigate wild type and mutant stem cells
46 migrating back and forth to the blood stream and calibrate the model based on murine
47 data.

48 Mutations in the DNA of the stem cells may be uncritical for hematopoiesis (neu-
49 tral/passenger mutations) or they may be critically disturbing (driver mutations), giv-
50 ing rise to blood cancer characterized by an overproduction of malfunctioning mature
51 cells - so-called transformed cells, which increase the risk of thrombosis [29]. Of spe-
52 cial interest is the *BCR-ABL1* kinase translocation (the Philadelphia chromosome) as a
53 driver for chronic myeloid leukemia, which has been studied using mathematical modelling
54 [44, 62, 65, 4, 15, 16, 32, 36, 49, 48, 56, 57]. However, the focus of the present paper is the
55 type of blood cancers denoted Philadelphia-negative myeloproliferative neoplasms (MPNs)
56 including essential thrombocytosis, polycythemia vera and primary myelofibrosis. These
57 are stem cell disorders evolving on a time scale of years characterized by acquired few driver
58 mutations, where *JAK2V617F* (*JAK2*) is the most common [60].

59 Few previous studies have addressed mathematical modelling of human MPNs. Zhang
60 et al. [74] recently investigated a model of MPNs with inflammation as a fixed, constant
61 input. Andersen et al. [1] proposed a more comprehensive model of human MPN develop-
62 ment that is the starting point for the present paper. *JAK2* mutated cells are explicitly

63 included at stem cell and mature cell level. As dynamical variables we include hematopoi-
64 etic and cancer stem cells that battle through a stem cell niche interaction, hematopoietic
65 and cancer mature cells, dead cells and inflammation level. This allows for investigation
66 of several intricate couplings: How does the population of hematopoietic and cancer stem
67 cells evolve and interact and how does this depend on the remaining part of the system? Is
68 cancer development aligned with development of increasing inflammation and vice versa,
69 is increasing inflammation positively or negatively affecting cancer progression? Which
70 mechanisms should be altered to stop further disease progression or ultimately cure the
71 patient? The long term behaviour of trajectories is investigated by a thorough analysis
72 of attractors of the system elucidating conditions and intervention strategies for cancer
73 escape, elimination, or equilibrium. In [51] the model is extended with T-cell response.
74 Here, we disregard this extension to allow for analytical investigation.

75 Section 2 presents the basic Cancitis model originally proposed in [1]. A useful quasi-
76 steady state approximation appears in section 2.1. In section 2.2 the system is transformed
77 into the clinically relevant variables and the equations are scaled and a comprehensive
78 analysis of the topology of the dynamics is presented. The model is compared to data and
79 discussed in section 3 along with various intervention strategies derived from the analysis of
80 the model. The structure of the transformed equations suggests that early cancer dynamics,
81 with and without treatment, can be captured by an explicit solution controlled by a single,
82 lumped parameter.

83 **2 Mathematical model of coupled blood production, blood** 84 **cancer and inflammation**

85 Figure 1 illustrates how hematopoiesis can be maintained on a systemic level. Hematopoi-
86 etic stem cells, x_0 , can self renew where a nonlinear inhibitory feedback accounts for limited
87 niche space, resources, and cytokine feedback. Stem cells may also differentiate through
88 multiple steps (represented by amplification factor, A) to mature blood cells, x_1 , here being
89 exemplified by the white blood cells (neutrophils). Both cell types may die, and debris of
90 the dead cells, a , is eliminated or recycled by the immune system, here lumped together in
91 one compartment, s , typically represented by cytokines associated with the immune system
92 activity such as IL- 1β , IL-1Ra, IL-2R, IL-8, IL-10, IL-12 and C-reactive protein. Excess of
93 dead cells leads to increased clearance by immune cells (red arrow). A need for extra or
94 fewer mature blood cells is thus mediated through the immune system [1],[51],[64].

95 In case of a stem cell mutation such as *JAK2*, figure 1 may be expanded with a stem
96 cell compartment of cancer stem cells, CSC (y_0), as well as mutated mature blood cells
97 (y_1) which is seen in figure 2, with corresponding equations (1), introduced by Andersen et
98 al. [1] inspired by the models of chronic myeloid leukemia by Dingli and Michor [10] and
99 by Stiehl et al. [61].

100 The introduction of mutated cells implies a competition at stem cell level where the

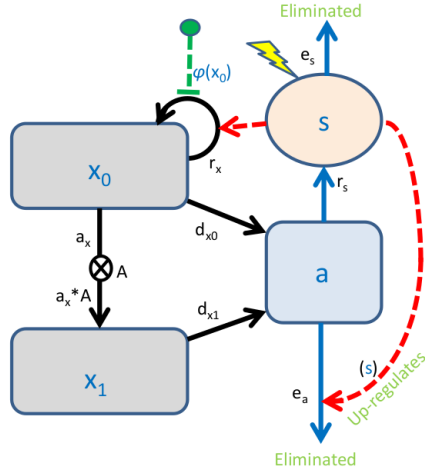


Figure 1: Blood production in a healthy individual is regulated by hematopoietic stem cells (x_0) that self renew with rate r_x regulated by a stem cell niche feedback, $\phi(x_0)$ and cytokine feedback (red arrow from s compartment) or differentiate with rate a_x in multiple steps (illustrated by amplification A) to ultimately becoming hematopoietic mature cells (x_1). HSC die with rate d_{x0} and mature blood cells die with rate d_{x1} . Dead cells (a) are engulfed by the immune system that here is pooled together in one compartment (s) that stimulates clearing of dead cells with rate e_a . Presence of dead cells stimulate immune cells with rate r_s . Endotoxins, smoking and other environmental factors may add to the inflammatory response, thus we add such a term (characterized by the lightning symbol).

101 HSC and CSC compete for space and nutrients in the bone marrow niche. Hematopoietic
102 stem cells are characterized by a self renewal rate, r_x , death rate, d_{x0} , and differentiation
103 into progeny, a_x . An inhibitory feedback, $\phi_x(x_0, y_0)$, from the stem cell niche takes into
104 account the limited space and nutrient supply and the competition between HSC and
105 CSC. Inflammation stimulates self renewal of stem cells [33] which is motivated by death
106 of mature healthy cells and provides a demand for replacement by new ones. Hence, the
107 effective self renewal is chosen as $r_x\phi_x(x_0, y_0)s$. Finally, HSC may mutate to become
108 CSC with rate r_m . The chance of mutation is believed to increase with inflammation
109 [26, 24, 9, 8, 37, 27, 71, 69, 72, 74, 22, 23] justifying an effective mutation rate being r_ms .

110 Proliferating stem cells go through a sequence of cell divisions to ultimately become
111 mature, differentiated cells. As we do not account for all intermediate division steps, the
112 growth rate of mature blood cells is a_x multiplied with amplification factor, A_x . The
113 mature cells undergo apoptosis with rate d_{x1} . Differential equations for CSC and cancer
114 mature cells are described similar to their healthy counterparts.

115 The apoptosis compartment is a collection of all cells that have undergone apoptosis and
116 is therefore positively stimulated by cells from other compartments with this destiny and
117 negatively affected by clearing by the immune cells, which is happening through a second
118 order mechanism - dead cells encountering immune cells are eliminated with a second order
119 rate e_a .

120 The immune system activity level is exemplified by cytokines such as IL 6 or IL 8 that
121 are inflammation markers related to hematological malignancies [8]. The complexity of the
122 immune system is assumed to be simplified due to a fast immune response compared to
123 the remaining dynamics resulting in a single, dynamical variable, s .

124 The immune level activity is stimulated by the presence of dead cells and has a self
125 elimination proportional to the population size. Further, an exogenous immune stimulation
126 is possible through $I(t)$ such as microbial infection and inflammation (e.g. smoking and
127 pollution). The resulting differential equations are shown in (1).

$$x'_0 = (r_x\phi_x s - d_{x0} - a_x)x_0 - r_msx_0 \quad (1a)$$

$$x'_1 = a_xA_xx_0 - d_{x1}x_1 \quad (1b)$$

$$y'_0 = (r_y\phi_y s - d_{y0} - a_y)y_0 + r_msx_0 \quad (1c)$$

$$y'_1 = a_yA_yy_0 - d_{y1}y_1 \quad (1d)$$

$$a' = d_{x0}x_0 + d_{y0}y_0 + d_{x1}x_1 + d_{y1}y_1 - e_aas \quad (1e)$$

$$s' = r_sa - e_ss + I(t) \quad (1f)$$

$$\phi_x = \phi_x(x_0, y_0) = \frac{1}{1 + (c_{xx}x_0 + c_{xy}y_0)^2} \quad (1g)$$

$$\phi_y = \phi_y(x_0, y_0) = \frac{1}{1 + (c_{yx}x_0 + c_{yy}y_0)^2}. \quad (1h)$$

129 As the model is inspired by Dingli and Michor [10], the default parameter values should
130 be comparable to theirs. The cell numbers are chosen as typical numbers for a human.
131 Prior to the first cancer stem cell, the model should be in steady state with 10^{10} mature
132 blood cells (the neutrophil count, similar approach as in [61]), and 10^4 HSC which is a
133 compromise between different reported values [21], [19], [61], [63], [10]. For a lifetime of
134 one week in tissue, we chose $d_{x1} = 0.1$ per day [52]. The effective self renewal of stem cells
135 $r_x \phi_x s$ is chosen to match cell division once per year.

136 The inflammatory level, s , is an abstract, scalable quantity whose progression which
137 correlate with the inflammation markers IL-1 β , IL-1Ra, IL-2R, IL-8, IL-10, IL-12 and C-
138 reactive protein. Production of dead cells are correlated with plasma lactic dehydrogenase,
139 see [1] including supplementary material for further details.

140 We expect $r_y > r_x$ for a blood cancer to develop, typically of measurable size after
141 5-10 years. For simplicity, we let unknown cancer cell parameter values equal their healthy
142 counterpart. To satisfy the above conditions, the default parameter values in table 1 are
143 obtained. For further details on parameter estimation for this model, see [1].

144 The mutant rate is set to default value $2 \cdot 10^{-8}$ such that expansion of CSC is driven by
145 mutations for CSC-values less than 1 and the CSC expansion is dominated by self renewal
146 for CSC larger than 1. As the mutation rate increases with inflammation [41], [25] the
147 effective mutation rate is included as $r_m s$. In the further analysis we both investigate the
148 effect of a continuous mutation corresponding to $r_m > 0$ and to a single event mutation
149 corresponding to initializing the model with a single cancer cell but letting $r_m = 0$.

Parameter	Value	Unit	Parameter	Value	Unit
r_x	$8.7 \cdot 10^{-4}$	day $^{-1}$	r_y	$1.3 \cdot 10^{-3}$	day $^{-1}$
a_x	$1.1 \cdot 10^{-5}$	day $^{-1}$	a_y	$1.1 \cdot 10^{-5}$	day $^{-1}$
A_x	$3.7 \cdot 10^{10}$	-	A_y	$3.7 \cdot 10^{10}$	-
d_{x0}	$2 \cdot 10^{-3}$	day $^{-1}$	d_{y0}	$2 \cdot 10^{-3}$	day $^{-1}$
d_{x1}	0.1	day $^{-1}$	d_{y1}	0.1	day $^{-1}$
c_{xx}	$7.5 \cdot 10^{-5}$	-	c_{yy}	$7.5 \cdot 10^{-5}$	-
c_{xy}	c_{xx}	-	c_{yx}	c_{yy}	-
e_s	2	day $^{-1}$	r_s	$3 \cdot 10^{-4}$	day $^{-1}$
e_a	$1.6 \cdot 10^6$	day $^{-1}$	I	7	day $^{-1}$
r_m	0 or $2 \cdot 10^{-8}$	day $^{-1}$			

Table 1: Default parameter values of model (1) given as total cells per human (a male of weight 70 kg).

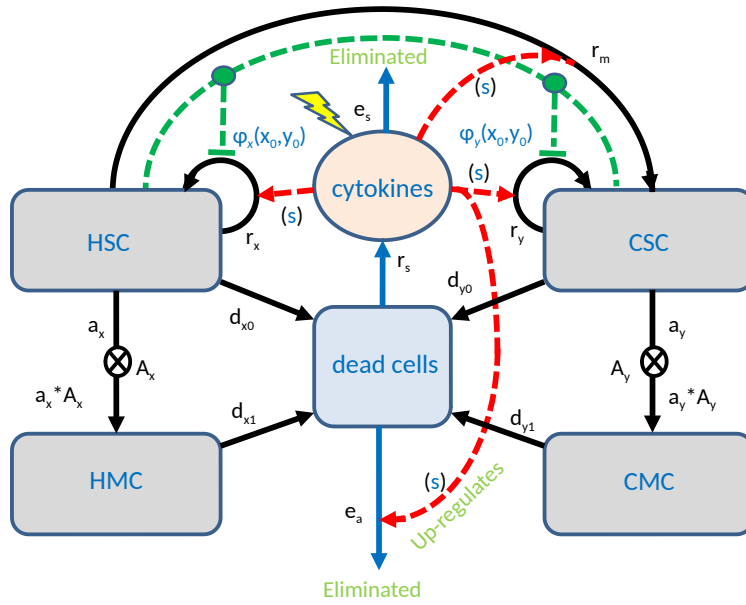


Figure 2: The hematopoiesis-cancer-inflammation model consists of six cell populations; the hematopoietic stem cells (HSC), the hematopoietic mature cells (HMC), the cancer stem cells (CSC), and the cancer mature cells (CMC), dead cells and cytokines. The mechanisms described in figure 1 are included also for cancer cells. HSC mutates with rate r_m to become CSC. The stem cell niche feedbacks, ϕ_x and ϕ_y now depend on both CSC and HSC to comply with the competition for space and growth signals.

150 **2.1 The simple cancitis model**

151 The dynamics of cytokine regulation is fast compared to blood production [65]. Further-
 152 more, white blood cells in the blood stream have a lifetime of six hours [70] to a week
 153 [52], while hematopoietic stem cells divide about once per year [11]. Therefore, we insist
 154 on mature cells and immune cells to be quickly equilibrated with the stem cell dynamics
 155 leading to the quasi steady state assumption

$$x'_1 = y'_1 = a' = s' = 0, \quad (2)$$

156 and with constant I making the system autonomous.

This leads to a two dimensional coupled ode-system, the *simple Cancitis model* (see appendix 4 for detailed derivation)

$$x'_0 = (r_x \phi_x s - d_{x0} - a_x) x_0 - r_m s x_0 \quad (3a)$$

$$y'_0 = (r_y \phi_y s - d_{y0} - a_y) y_0 + r_m s x_0 \quad (3b)$$

$$x_1 = \frac{a_x A_x}{d_{x1}} x_0 \quad (3c)$$

$$y_1 = \frac{a_y A_y}{d_{y1}} y_0 \quad (3d)$$

$$s = \frac{I}{2e_s} + \sqrt{\left(\frac{I}{2e_s}\right)^2 + \frac{r_s (a_x A_x + d_{x0})}{e_a e_s} \left(x_0 + \frac{a_y A_y + d_{y0}}{a_x A_x + d_{x0}} y_0\right)} \quad (3e)$$

$$a = -\frac{I}{2r_s} + \frac{e_s}{r_s} \sqrt{\left(\frac{I}{2e_s}\right)^2 + \frac{r_s (a_x A_x + d_{x0})}{e_a e_s} \left(x_0 + \frac{a_y A_y + d_{y0}}{a_x A_x + d_{x0}} y_0\right)} \quad (3f)$$

$$\phi_x = \phi_x(x_0, y_0) = \frac{1}{1 + (c_{xx} x_0 + c_{xy} y_0)^2} \quad (3g)$$

$$\phi_y = \phi_y(x_0, y_0) = \frac{1}{1 + (c_{yx} x_0 + c_{yy} y_0)^2}. \quad (3h)$$

157 Allowed initial values of (x_0, y_0) belong to $\mathcal{D}_1 = \mathbb{R}^+ \cup \{0\} \times \mathbb{R}^+ \cup \{0\}$. The parameter
 158 values are non negative so \mathcal{D}_1 is invariant to the flow defined by equation (3).

159 Using default parameter values, system (3) is an excellent approximation to system
 160 (1) - see figure 3. To test the robustness, parameter values and initial conditions are
 161 varied and 100 simulations were performed. All initial conditions and parameters (except
 162 r_x, d_{x1}, A_x, e_s) are chosen from a normal distribution with mean given by the default value
 163 and standard deviation being 25% of the default value. If a negative value is sampled,
 164 then the value is discarded and a new sample is taken. The parameters r_x, d_{x1}, A_x, e_s
 165 are then chosen such that the system is initiated at the hematopoietic steady state for
 166 mutation rate $r_m = 0$ and no initial cancer cells present. The full model and the simple
 167 model are evaluated daily for 80 years. The difference for each variable, x_0, x_1, y_0, y_1, a, s

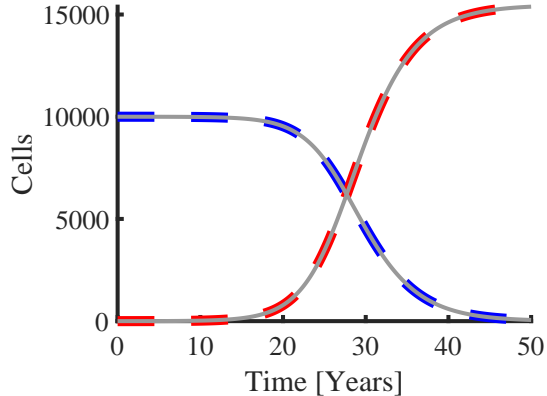


Figure 3: Comparison of the full model (1) and the simple model (3) using default parameter values. Blue curve is the number of hematopoietic stem cells, red curve is number of cancer stem cells using the full model. Grey curves are the corresponding quantities in the reduced model.

168 is computed and normalized by the initial value except y_0 and y_1 which are normalized
 169 by their hematopoietic counterpart. The maximum distance is then computed as the
 170 maximum deviation i.e. using the L^∞ norm. Due to the normalization, the distance is a
 171 dimension free number. The distance is less than 0.004 for all variables for all simulations,
 172 which means there is no visual difference in plots such as observed in figure 3. Hence, the
 173 difference between the full and simple model scaled by the baseline value is at any point in
 174 time less than one percent so the reduced model is a good approximation to the full model
 175 in all investigated cases.

176 2.2 Reformulating the simple model using the total white blood cells 177 and *JAK2* allele burden

The simple model can be formulated as a closed system of x_1 and y_1 using the proportionality between x_0 and x_1 and between y_0 and y_1 . Excluding $(x_1, y_1) = (0, 0)$ we can define the coordinate transformation $\mathcal{D}_1 \setminus \{(0, 0)\} \rightarrow \mathbb{R}^+ \times [0, 1]$, $(x_1, y_1) \rightarrow (z_1, z_2)$ where $z_1 \in \mathbb{R}^+$ is the total number of white blood cells and $z_2 \in [0, 1]$ is the *JAK2* allele burden. Thus we exclude the trivial possibility of having no mature cells corresponding to $z_1 = 0$.

$$z_1 = x_1 + y_1 \tag{4a}$$

$$z_2 = \frac{y_1}{x_1 + y_1} \tag{4b}$$

with inverse mapping

$$x_1 = z_1(1 - z_2) \quad (5a)$$

$$y_1 = z_1 z_2. \quad (5b)$$

This means that the clinically, measurable quantities are explicitly modelled as the only dynamic variables. Some parameters are difficult to assess, so for simplicity some parameters of the healthy cells and the cancer cells are chosen to be equal. Following [1] we investigate the case with the constraints

$$a_x = a_y \quad (6a)$$

$$A_x = A_y \quad (6b)$$

$$d_{x0} = d_{y0} \quad (6c)$$

$$d_{x1} = d_{y1} \quad (6d)$$

$$c_{xx} = c_{yy}. \quad (6e)$$

178 An analysis relaxing equation (6) is omitted here due to the parsimonious principle and
179 lack of data.

180 The equations of total number of white blood cells and allele burden from equation (4)
181 and equation (3) then simplifies to

$$z_1' = z_1 \left((r_x + z_2(r_y - r_x)) \tilde{\phi} \tilde{s} - d_{x0} - a_x \right) \quad (7a)$$

$$z_2' = (1 - z_2) \left(z_2(r_y - r_x) \tilde{\phi} + r_m \right) \tilde{s} \quad (7b)$$

$$\tilde{\phi} = \frac{1}{1 + \left(c_{xx} \frac{d_{x1}}{a_x A_x} \right)^2 z_1^2} \quad (7c)$$

$$\tilde{s} = \frac{I}{2e_s} + \sqrt{\left(\frac{I}{2e_s} \right)^2 + \frac{d_{x1}}{a_x A_x} \frac{r_s (a_x A_x + d_{x0})}{e_a e_s} z_1}. \quad (7d)$$

182 Then hypotheses based on clinical data can be directly investigated in the model and vice
183 versa that features in the model may give rise to hypotheses that may be tested from
184 appropriate clinical data. We will study system (7) with $z_1 \geq 0$ and $0 \leq z_2 \leq 1$. In
185 particular, we will allow $z_1 = 0$ in the subsequent analysis even though the coordinate
186 transformation $(x_1, y_1) \leftrightarrow (z_1, z_2)$ is not defined here. The differential equations (7) can
187 easily be defined for $z_1 = 0$, and the stability of fixed points on the line $z_1 = 0$ provide
188 information on phase space for $z_1 > 0$ where the coordinate transformation is well defined.

189 For $z_2(0) \in [0, 1]$, $z_2(t)$ stays within this interval as $(1 - z_2)$ is a factor in z_2' and for
190 $z_2 = 0$, $z_2' \geq 0$. From equation (7a) we see that $\tilde{\phi} \tilde{s}$ is going to 0 for z_1 approaching infinity
191 implying there exists a number M such that for $z_1 > M$ then $\dot{z}_1 < 0$. For non negative
192 initial conditions, $z_1(t)$ stays non negative (as $z_1 = 0$ is a z_1 null cline). Therefore, the
193 compact set $[0, M] \times [0, 1]$ is an *attracting trapping region* for the system.

194 **2.3 Scaled equations**

195 A scaled form of equation (7) is now formulated to facilitate further analysis. We introduce
 196 a constant \bar{z} (value to be determined) and a variable, Z_1 , such that

$$z_1 = \bar{z}Z_1. \quad (8)$$

197 Similarly, we introduce the dimensionless time τ by

$$t = \bar{t}\tau, \quad (9)$$

198 where \bar{t} is a constant to be determined. Then, differential equations of Z_1 and z_2 can be
 199 formulated from equation (8), equation (9) and equation (7) with the notation $\dot{z} = \frac{dz}{d\tau}$.
 200 From the chain rule and equation (8)

$$\dot{Z}_1 = \frac{\bar{t}}{\bar{z}}z'_1. \quad (10)$$

201 Inserting the expression for z'_1 from equation (7a) along with equation (8) we obtain

$$\dot{Z}_1 = \bar{t}Z_1 \left((r_x + z_2(r_y - r_x))\tilde{\phi}\tilde{s} - d_{x0} - a_x \right) \quad (11)$$

202 with

$$\tilde{\phi}\tilde{s} = \frac{I}{2e_s} \frac{1 + \sqrt{1 + 4e_s d_{x1} r_s \frac{a_x A_x + d_{x0}}{I^2 a_x A_x e_a} \bar{z} Z_1}}{1 + \left(\frac{c_{xx} d_{x1}}{a_x A_x} \right)^2 \bar{z}^2 Z_1^2} \quad (12)$$

203 To simplify the denominator, we choose

$$\bar{z} = \frac{a_x A_x}{c_{xx} d_{x1}} \quad (13)$$

204 denoting the lumped parameter expression in the numerator by β_1 ,

$$\beta_1 = 4 \frac{e_s r_s}{c_{xx} e_a I^2} (a_x A_x + d_{x0}), \quad (14)$$

205 equation (11) becomes

$$\dot{Z}_1 = \bar{t}Z_1 \left(r_x \frac{I}{2e_s} \left(1 + z_2 \left(\frac{r_y}{r_x} - 1 \right) \right) \frac{1 + \sqrt{1 + \beta_1 Z_1}}{1 + Z_1^2} - d_{x0} - a_x \right). \quad (15)$$

206 By choosing

$$\bar{t} = \frac{2e_s}{r_x I}, \quad (16)$$

the first term is simplified, and we may conveniently introduce two lumped parameters, β_2 and β_3 by

$$\beta_2 = \frac{r_y}{r_x} - 1 \quad (17a)$$

$$\beta_3 = 2 \frac{e_s}{r_x I} (d_{x0} + a_x) . \quad (17b)$$

207 For \dot{z}_2 the equation then becomes

$$\dot{z}_2 = \bar{t} z'_2 = (1 - z_2) \frac{1 + \sqrt{1 + \beta_1 Z_1}}{1 + Z_1^2} \left(\beta_2 z_2 + \frac{r_m}{r_x} (1 + Z_1^2) \right) \quad (18)$$

208 which suggests a fourth lumped parameters as

$$\beta_4 = \frac{r_m}{r_x} . \quad (19)$$

In summary, we obtain the system

$$\dot{Z}_1 = Z_1 \left((1 + \beta_2 z_2) \frac{1 + \sqrt{1 + \beta_1 Z_1}}{1 + Z_1^2} - \beta_3 \right) \quad (20a)$$

$$\dot{z}_2 = (1 - z_2) \frac{1 + \sqrt{1 + \beta_1 Z_1}}{1 + Z_1^2} (\beta_2 z_2 + \beta_4 (1 + Z_1^2)) , \quad (20b)$$

with new parameters given by relations to the old ones

$$\beta_1 = 4 \frac{e_s r_s}{c_{xx} e_a I^2} (a_x A_x + d_{x0}) \quad (21a)$$

$$\beta_2 = \frac{r_y}{r_x} - 1 \quad (21b)$$

$$\beta_3 = 2 \frac{e_s}{r_x I} (d_{x0} + a_x) \quad (21c)$$

$$\beta_4 = \frac{r_m}{r_x} . \quad (21d)$$

209 The equations (20) describe the mature cells (Z_1) in reduced units (equation (8)) and allele
 210 burden (z_2) progression over time, with parameters related to stem cell, mature cell and
 211 immune system mechanisms. Parameters are constrained by $\beta_1, \beta_3 > 0$ and $\beta_4 \geq 0$ and
 212 $\beta_2 \geq -1$, with default parameter values in table 2 computed from the default parameters of
 213 the full model, table 1. The parameter β_2 is related solely to the stem cell compartments,
 214 with negative values if $r_x > r_y$ and positive values if $r_x < r_y$. The parameter β_4 is the
 215 mutation rate relative to the hematopoietic self renewal rate. The value of this parameter
 216 will also be investigated when equal to zero, to allow for a one hit mutation (by setting the
 217 initial condition to one cancer cell) instead of considering a continuous mutation rate. The

β_1	β_2	β_3	β_4
0.16	0.48	1.32	$2.3 \cdot 10^{-5}$

Table 2: Default parameter values of system (21).

parameters β_1 and β_3 provide nontrivial connection between original system parameters related to the immune cells, dead cells, stem cells and mature cells. β_3 is the product of two lumped parameters that are important for cell exhaustion namely a loss versus production term on stem cell level, $\frac{a_x+d_0}{r_x}$, and a loss versus production term at immune cell level, $\frac{e_s}{I}$.

Regarding β_1 , the presence of $a_x A_x$ implies that an increase in proliferation signal increase the β_1 - value. An increased strength of the niche feedback (increasing c_{xx}) leads to a decreased β_1 . Except for c_{xx} , the original parameters entering β_1 relates to the value of apoptotic cells and immune cells for a given number of stem cells - see equation (3e) and (3f), as a ratio between effects that increase a and s levels namely $\frac{r_s}{e_a e_s} (a_x A_x + d_{x0})$ and $\left(\frac{I}{e_s}\right)^2$.

2.4 Phase space analysis

The reduction from six differential equations to two has several useful implications. The order of the phase space is reduced from six to two allowing visualizations using the phase plane giving an overview of trajectories for many initial conditions simultaneously. The two-dimensional dynamics is quite restricted since trajectories cannot cross as the existence and uniqueness theorem applies. In the reduced model, the parameters of the full system are grouped in the parameters β_1, \dots, β_4 showing the minimum number of parameters giving a functional dependence on the original parameters that otherwise would have shown up as correlated. The simplicity of system (20) implies that significant analysis can be conducted which is the focus of the current section. To categorize the steady states satisfying $\dot{Z}_1 = \dot{z}_2 = 0$ we employ the following vocabulary:

- A *hematopoietic steady state* is defined as having $z_2 = 0$.
- A *cancer steady state* is defined as having $z_2 = 1$.
- A *co-existing steady state* is defined as having $0 < z_2 < 1$.

A cancer steady state always exists with value $(Z_1, z_2) = (0, 1)$. For $\beta_4 = 0$ also $(Z_1, z_2) = (0, 0)$ is a trivial steady state solution.

2.4.1 Analytic bound on trapping region

The existence of a trapping region is already established. An analytic expression of an upper bound of Z_1 at the trapping region boundary is formulated. Consider equation (20a) for $Z_1 \geq 1$ implying $0 < Z_1^{-1} \leq 1$,

$$\begin{aligned}
(1 + \beta_2 z_2) \frac{1 + \sqrt{1 + \beta_1 Z_1}}{1 + Z_1^2} - \beta_3 &\leq (1 + |\beta_2|) \frac{Z_1^{-1} + \sqrt{Z_1^{-2} + \beta_1 Z_1^{-1}}}{Z_1^{-1} + Z_1} - \beta_3 \\
&\leq (1 + |\beta_2|) \frac{1 + \sqrt{1 + \beta_1}}{Z_1} - \beta_3.
\end{aligned} \tag{22}$$

248 Solving for Z_1 requiring the latter expression being negative, an upper bound on the
249 trapping region in the Z_1 direction is obtained,

$$M_1 = \max\left\{1, (1 + |\beta_2|) \frac{1 + \sqrt{1 + \beta_1}}{\beta_3}\right\} = (1 + |\beta_2|) \frac{1 + \sqrt{1 + \beta_1}}{\beta_3}, \tag{23}$$

250 For $\beta_2 < 0$, $|1 + \beta_2 z_2| \leq 1$, providing the smaller bound

$$M_2 = \max\left\{1, \frac{1 + \sqrt{1 + \beta_1}}{\beta_3}\right\}. \tag{24}$$

251 Hence, an attractive trapping region is $M_1 \times [0, 1]$ for $\beta_2 > 0$ and $M_2 \times [0, 1]$ for $\beta_2 < 0$.
252 This implies that solutions initially located outside the trapping region is attracted to it,
253 and any solution once in the trapping region will stay there. A consequence of this is that
254 the trajectories exist globally in time [55].

255 The possible dynamics in bounded, two-dimensional flow is very limited as the only
256 attractors are fixed points or limit cycles. We restate the Poincaré Bendixon theorem as
257 stated in for example [54].

258 **Theorem 1 (Poincaré-Bendixon)** *Given a system of ordinary differential equations $\frac{dx}{dt} =$
259 $F(x)$, where x is two dimensional, let $x(t)$ represent a solution trajectory of the system
260 which is bounded. Then either $x(t)$ converges as $t \rightarrow \infty$ to an equilibrium point of the
261 system, or it converges to a periodic cycle.*

262 **Remark 1** *Due to index theory [47], any periodic solution in a two-dimensional phase
263 space must have at least one fixed point in its interior. Therefore, if no coexistence steady
264 states exist, then no limit cycles can exist. From monotonicity properties of equation
265 (20b), $\dot{z}_2 = 0$ only allows for coexistence points and limit cycles if $\beta_2 < 0$ and $\beta_4 > 0$ i.e.
266 if HSC self renewal dominates CSC self renewal and new CSC are continuously produced
267 by mutations.*

268 All steady state solutions are roots of a polynomial of at most fifth order which easily
269 can be solved numerically using standard software. As an example, consider the nontrivial
270 cancer steady state satisfying $z_2 = 1$ and Z_1 being the solution of

$$0 = \left((1 + \beta_2) \frac{1 + \sqrt{1 + \beta_1 Z_1}}{1 + Z_1^2} - \beta_3 \right) \tag{25}$$

271 corresponding to

$$\sqrt{1 + \beta_1 Z_1} = \frac{\beta_3}{1 + \beta_2} (1 + Z_1^2). \quad (26)$$

272 Squaring this expression gives a fourth order polynomial.

$$0 = \left(\frac{\beta_3}{1 + \beta_2}\right)^2 Z_1^4 + 2 \left(\frac{\beta_3}{1 + \beta_2}\right)^2 Z_1^2 - \beta_1 Z_1 + \left(\frac{\beta_3}{1 + \beta_2}\right)^2 - 1. \quad (27)$$

273 All roots can then easily be computed numerically for a given set of parameter values.
 274 Then, the relevant, physiological solutions must be real, satisfy $Z_1 > 0$ and fulfill equation
 275 (26). This approach implies that all critical points can be numerically computed. The
 276 local stability of a steady state can then be computed by evaluating the eigenvalues of the
 277 Jacobian at the steady state, provided that the steady state is hyperbolic. Some phase
 278 planes corresponding to different parameter values are shown in figure 4. The following
 279 analysis address the typical phase plane topologies depending on the parameter values.

280 2.4.2 Hematopoiesis

281 We first consider hematopoiesis (figure 1) by expecting a stable, positive equilibrium of

$$\dot{Z}_1 = Z_1 \left(\frac{1 + \sqrt{1 + \beta_1 Z_1}}{1 + Z_1^2} - \beta_3 \right). \quad (28)$$

282 Defining

$$F(Z_1) = \frac{1 + \sqrt{1 + \beta_1 Z_1}}{1 + Z_1^2}, \quad (29)$$

283 a fixed point of \dot{Z}_1 for non zero Z_1 then requires $F(Z_1) - \beta_3 = 0$. The monotonicity
 284 properties of F are important for the further analysis. F is an increasing function of Z_1
 285 for small, positive values, then it has a unique maximum at $Z_1 = \tilde{Z}_1$, and is decreasing for
 286 $Z_1 > \tilde{Z}_1$. $F(0) = 2$, and F goes to 0 for large Z_1 . This implies that for $\beta_3 < 2$, a unique,
 287 positive solution exists to $F(Z_1) - \beta_3 = 0$. Since $F(0) - \beta_3 > 0$, then $F(Z_1) - \beta_3$ cross zero
 288 with negative slope so the steady state is stable [47].

289 For $2 < \beta_3 < F(\tilde{Z}_1)$ exactly two steady state positive solutions exist. The first steady
 290 state occurs where $F(Z_1) - \beta_3$ has positive slope, causing the steady state to be unstable,
 291 while the steady state with largest Z_1 value occurs where $F(Z_1) - \beta_3$ has negative slope,
 292 causing the steady state to be stable. For $\beta_3 > F(\tilde{Z}_1)$ no steady state solutions exists. A
 293 sufficient criterion for this is $\beta_3 > 1 + \sqrt{1 + \beta_1^2}$. The parameter region allowing for two
 294 hematopoietic steady states is small. Biologically, an upper bound on β_3 is meaningful for
 295 hematopoiesis as stem cell exhaustion is expected for large parameters related to removal
 296 of cells, $(d_{x0} + a_x)e_s$ and small parameters related to production of cells, $r_x I$. For the
 297 remaining part of the paper, we will focus on $\beta_3 < 2$ as this guarantees existence of
 298 a stable fixed point of equation (28). For the default parameter values this criterion is

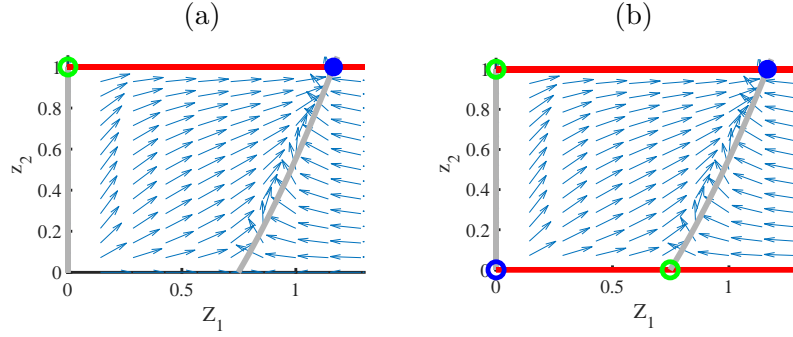


Figure 4: Phase space of equation (20) for $\beta_2 > 0$. Open blue circles are unstable steady states with both eigenvalues having positive real part, green open circles are saddles, closed circles are stable steady states, grey curves are null clines of \dot{Z}_1 , red curves are null clines of \dot{z}_2 . Default parameters are used in (a) where a cancer steady state attracts all trajectories with $Z_1(0) > 0$, satisfying lemma 1. In (b), default parameter values are used except $\beta_4 = 0$, so lemma 2 applies showing a cancer steady state attracts trajectories with initial conditions $Z_1(0) > 0$ and $0 < z_2(0) < 1$.

299 fulfilled. For $\beta_3 < 2$ the unique, positive root of $F(Z_1) - \beta_3 = 0$ is denoted \bar{Z}_1 , which
 300 has value 0.75 for default parameter values. An increase in β_1 shifts the equilibrium blood
 301 cell count to higher values and an increase in β_3 shifts the equilibrium blood cell to lower
 302 values as β_3 acts as an effective death rate of mature cells. In terms of original parameters
 303 this means that an increase in r_s or A_x increase the equilibrium blood cell number, while
 304 an increase in c_{xx} or e_a decrease the equilibrium blood cell number.

305 As $\dot{Z}_1 < 0$ for $Z_1 > \bar{Z}_1$, $[0; \bar{Z}_1] \times [0, 1]$ is a trapping region. We now systematically
 306 investigate the phase plane topologies of equation (20). When possible, the results are
 307 summarized in lemmas and phase plane figures, which may be conducted for a fast overview
 308 of the possible dynamics of the model.

309 2.4.3 The case $\beta_2 > 0$

310 Consider the case $\beta_2 > 0$ corresponding to $r_y > r_x$. First, we assume $\beta_4 > 0$, which
 311 prevents hematopoietic steady states since $\dot{z}_2 > 0$ for $z_2 = 0$. In this case, the only zero of
 312 \dot{z}_2 is for $z_2 = 1$ i.e. a cancer steady state, hence neither hematopoietic steady states nor
 313 coexistence points are possible for $\beta_2 > 0$, $\beta_4 > 0$. The criterion $\dot{Z}_1 = 0$ with $Z_1 \neq 0$ and
 314 $z_2 = 1$ is

$$0 = F(Z_1) - \frac{\beta_3}{1 + \beta_2}, \quad (30)$$

315 which has a unique solution for $\beta_3 < 2$ by similar arguments as for the hematopoiesis
 316 investigation. Solutions to equation (30) solves

$$0 = \left(\frac{\beta_3}{1 + \beta_2} \right)^2 Z_1^4 + 2 \frac{\beta_3}{1 + \beta_2} \left(\frac{\beta_3}{1 + \beta_2} - 1 \right) Z_1^2 - \beta_1 Z_1 + \frac{\beta_3}{1 + \beta_2} \left(\frac{\beta_3}{1 + \beta_2} - 2 \right). \quad (31)$$

317 The first coefficient is positive and the third is negative. Hence, regardless of the sign of
 318 the second coefficient, there is one sign change from the first to the third coefficient. As
 319 $\beta_2 \geq 0$, $0 < \beta_3 < 2$ then $\frac{\beta_3}{1 + \beta_2} - 2 \leq \beta_3 - 2 < 0$, hence the last term is negative, and the
 320 sequence of coefficients in equation (31) has one sign change for $\beta_2 \geq 0$ and $\beta_3 < 2$, so
 321 there is a unique solution to $\dot{Z}_1 = 0$ for $Z_1 > 0$ in this case. Denote this value by Z_1^* . In
 322 summary, for $\beta_2 \geq 0, \beta_4 > 0$ and $0 < \beta_3 < 2$ there are two fixed points: $(0, 1)$ and $(Z_1^*, 1)$.
 323 Consider equation (20a) for any $z_2 \in [0; 1]$:

$$\lim_{Z_1 \rightarrow 0^+} \frac{\dot{Z}_1}{Z_1} = 2(1 + \beta_2 z_2) - \beta_3 \geq 2 - \beta_3 > 0. \quad (32)$$

324 This implies that the fixed point $(0, 1)$ is unstable and that we may choose any small $\epsilon > 0$
 325 such that for $Z_1 = \epsilon$ then $\dot{Z}_1 > 0$ for any $z_2 \in [0; 1]$. The trapping region

$$T_1 = [\epsilon; M_1] \times [0; 1] \quad (33)$$

326 only contains one fixed point, namely $(Z_1^*, 1)$. As there can be no limit cycles, we have
 327 proved the following lemma.

328 **Lemma 1** *For $\beta_2 \geq 0, \beta_4 > 0$ and $\beta_3 < 2$ there are two fixed points of equation (20), $(0, 1)$
 329 and $(Z_1^*, 1)$. $(Z_1^*, 1)$ attracts all solutions with $Z_1(0) > 0$.*

330 For $\beta_2 > 0$ and $\beta_4 = 0$ there are additional two critical points, at $(0, 0)$ and the
 331 hematopoietic steady state $(\bar{Z}_1, 0)$. As $\dot{z}_2 > 0$ for any $0 < z_2 < 1$ these two critical points
 332 are unstable. No coexistence points are possible. For any small $\epsilon > 0$ we define the set

$$T_2 = [\epsilon; M_1] \times [\epsilon; 1], \quad (34)$$

333 which is a trapping region. $(Z_1^*, 1)$ is the only attractor in T_2 and hence globally stable
 334 within T_2 .

335 The line $z_2 = 0$ is invariant to the flow, and trajectories on this line are attracted to
 336 $(\bar{Z}_1, 0)$ by similar reasoning as in section 2.4.2.

337 **Lemma 2** *For $\beta_2 > 0, \beta_4 = 0$ and $\beta_3 < 2$ there are four fixed points of equation (20),
 338 $(0, 0)$, $(0, 1)$, $(Z_1^*, 1)$, and $(\bar{Z}_1, 0)$. The cancer steady state $(Z_1^*, 1)$ attracts all solutions with
 339 $Z_1(0) > 0, z_2(0) > 0$. $(\bar{Z}_1, 0)$ attracts trajectories satisfying $z_2(0) = 0$ and $Z_1(0) > 0$.*

340 **2.4.4 The case $\beta_2 = 0$ and $\beta_4 = 0$**

341 Consider the case $\beta_2 = \beta_4 = 0$, $\beta_3 < 2$. The dynamics is very simple as $\dot{z}_2 = 0$ i.e. the
 342 allele burden does not vary with time. The dynamics of Z_1 then follows similar dynamics
 343 as for hematopoiesis, section 2.4.2 i.e. there are two zeros of \dot{Z}_1 , $Z_1 = 0$ and $Z_1 = \bar{Z}_1$. For
 344 any $Z_1(0) > 0$, Z_1 approaches \bar{Z}_1 .

345 Disease progression occurs with $\beta_2 > 0$ leading to a measurable *JAK2* allele burden
 346 which may be altered by a targeted drug leading to $\beta_2 = 0$ i.e. similar HSC and CSC self
 347 renewal. In this case, the mature blood cell count will be maintained at a healthy value,
 348 with a constant proportion of *JAK2* cells.

349 **2.4.5 The case $\beta_2 = 0$ and $\beta_4 > 0$**

350 In this case \dot{z}_2 is only zero for $z_2 = 1$, and is increasing for $z_2 \in [0, 1)$. There are two steady
 351 states, $(0, 1)$ is unstable and $(\bar{Z}_1, 1)$ is stable and attracts all solutions with $Z_1(0) > 0$.
 352 This corresponds to the cancer stem cells dominate due to mutational supply from the
 353 hematopoietic stem cells.

354 **2.4.6 The case $-1 < \beta_2 < 0$ and $\beta_4 = 0$**

355 We investigate the case $-1 < \beta_2 < 0$ corresponding to $r_x > r_y$ and $\beta_4 = 0$ i.e no continuous
 356 mutation rate. Steady states are located at $(0, 1)$, $(\bar{Z}_1, 0)$, $(0, 1)$ and there may be additional
 357 two cancer steady states, related to the monotony properties of F . If $\frac{\beta_3}{1+\beta_2} < 2$ or $\frac{\beta_3}{1+\beta_2} =$
 358 $F(\tilde{Z})$ there are two cancer steady states. If $2 < \frac{\beta_3}{1+\beta_2} < F(\tilde{Z})$ there are three cancer steady
 359 states. If $\frac{\beta_3}{1+\beta_2} > F(\tilde{Z})$ there is only the trivial cancer steady state, $(0, 1)$, see figure 5.

360 The former case is symmetric to the case $\beta_2 > 0$, $\beta_4 = 0$. For any small $\epsilon > 0$ the set
 361 $[\epsilon; M_1] \times [0; 1 - \epsilon]$ is a trapping region, that only contains one steady state, which is on the
 362 boundary of the set.

363 In the remaining cases, $[0; M_1] \times [0; 1 - \epsilon]$ is a trapping region i.e. the flow is repelled from
 364 the cancer steady states. The trivial steady state $(0, 0)$ is a saddle, with stable manifold
 365 along the z_2 axis, which is also invariant to the flow. Hence, also in this case does $(\tilde{Z}, 0)$
 366 attract initial conditions in $[\epsilon; M_1] \times [0; 1 - \epsilon]$.

367 **Lemma 3** For $-1 < \beta_2 < 0$, $\beta_4 = 0$ and $\beta_3 < 2$ the hematopoietic steady state $(\bar{Z}_1, 0)$
 368 attracts all trajectories with $Z_1(0) > 0$, $z_2(0) < 1$. Unstable steady states are $(0, 0)$, $(0, 1)$
 369 and if $2 < \frac{\beta_3}{1+\beta_2} < F(\tilde{Z})$ there are additional two unstable cancer steady states.

370 **2.4.7 The case $-1 < \beta_2 < 0$ and $\beta_4 > 0$**

371 In this case there are no hematopoietic steady states, as $\dot{z}_2 > 0$ for $z_2 = 0$. There may be
 372 zero, one or two cancer steady states, satisfying equation (30). Zeros of \dot{z}_2 are $z_2 = 1$ or

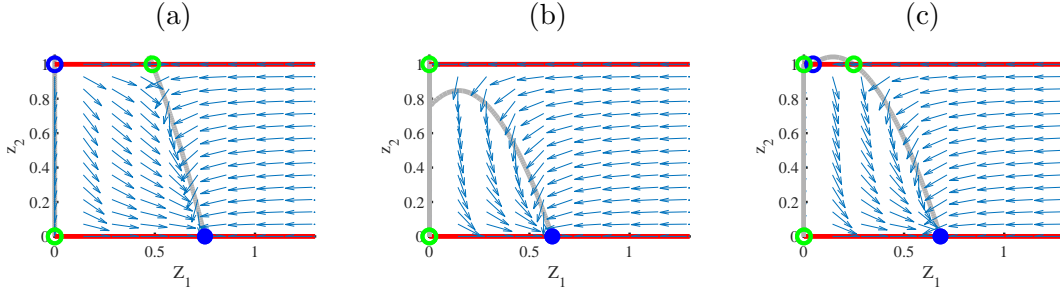


Figure 5: Phase space for $-1 < \beta_2 < 0$, $\beta_4 = 0$. In all cases $(\bar{Z}_1, 0)$ attracts all trajectories excluding initial condition $Z_1(0) = 0$ or $z_2(0) = 1$.

373 $z_2 = f_1(Z_1)$ with

$$f_1(Z_1) = -\frac{\beta_4}{\beta_2} (1 + Z_1^2) . \quad (35)$$

374 As f_1 is increasing with Z_1 , we may use equation (24) to get an upper bound on this null

375 cline within the Z_1 values of the trapping region. Then, f_1 has values in $[-\frac{\beta_4}{\beta_2}; -\frac{\beta_4}{\beta_2} \left(1 + \left(\frac{1+\sqrt{1+\beta_1}}{\beta_3}\right)^2\right)]$

376 within the Z_1 values of the trapping region.

377 The null clines of \dot{Z}_1 are $Z_1 = 0$ or $z_2 = f_2(Z_1)$ with

$$f_2(Z_1) = \frac{1}{-\beta_2} \left(1 - \frac{\beta_3}{F(Z_1)}\right) \quad (36)$$

378 For admissible z_2 values $1 > -\beta_2 > \beta_4 > 0$ is needed. The Jacobian evaluated at the
379 steady state $(0, -\frac{\beta_4}{\beta_2})$ is then

$$J \left(0, -\frac{\beta_4}{\beta_2}\right) = \begin{bmatrix} 2(1 - \beta_4) - \beta_3 & 0 \\ 0 & 2\beta_2 \left(1 + \frac{\beta_4}{\beta_2}\right) \end{bmatrix} , \quad (37)$$

380 The second eigenvalue is always negative, with corresponding eigen direction being the
381 z_2 axis. The sign of first eigenvalue $2(1 - \beta_4) - \beta_3$ then determines the stability properties.
382 By direct calculation, it is easily seen that the steady state is stable if $f_1(0) > f_2(0)$ and a
383 saddle if $f_1(0) < f_2(0)$ thus proving the following remark.

384 **Remark 2** A necessary condition for any coexistence steady state is $1 > -\beta_2 > \beta_4 >$
385 0 . This condition is also sufficient for a coexistence point located at the boundary of the
386 trapping region $(0, -\frac{\beta_4}{\beta_2})$. This steady state is a saddle with stable eigenvector along the
387 z_2 - axis if $2(1 - \beta_4) - \beta_3 > 0$ (corresponding to $f_1(0) < f_2(0)$), and a stable node if
388 $2(1 - \beta_4) - \beta_3 < 0$ (corresponding to $f_1(0) > f_2(0)$).

389 A cancer steady state $(Z_1^*, 1)$ with positive Z_1^* must satisfy $f_2(Z_1^*) = 1$ which is equivalent
 390 to $F(Z_1^*) = \frac{\beta_3}{1+\beta_2}$. Linear stability analysis provides knowledge of the type of steady state
 391 based on f_1 and f_2 in the generic cases.

392 **Lemma 4** *Let $-1 < \beta_2 < 0$, $\beta_4 > 0$, $0 < \beta_3 < 2$. If a cancer steady state exists with*
 393 *$f_2(Z_1^*) = 1$ it is*

- 394 • *a saddle if $f_2'(Z_1^*) > 0 \wedge f_1(Z_1^*) > 1$ or $f_2'(Z_1^*) < 0 \wedge f_1(Z_1^*) < 1$.*
- 395 • *an unstable node or focus if $f_2'(Z_1^*) > 0 \wedge f_1(Z_1^*) < 1$.*
- 396 • *a stable node or focus if $f_2'(Z_1^*) < 0 \wedge f_1(Z_1^*) > 1$.*

397 **PROOF.** The proof is based on direct computation of the trace and determinant of the
 398 Jacobian evaluated at the steady state, providing knowledge of the eigenvalues. If the
 399 determinant is negative, the steady state is a saddle. If the determinant is positive and
 400 the trace is positive, the steady state is an unstable node or focus. If the determinant is
 401 positive and the trace is negative, the steady state is a stable node or focus.

$$\det(J(Z_1^*, 1)) = -\beta_2 Z_1^* (1 + \beta_2) F'(Z_1^*) F(Z_1^*) (1 - f_1(Z_1^*)) \quad (38a)$$

$$\text{tr}(J(Z_1^*, 1)) = Z_1^* (1 + \beta_2) F'(Z_1^*) - \beta_2 F(Z_1^*) (1 - f_1(Z_1^*)) \quad (38b)$$

402 As $\text{sign}(F'(Z_1^*)) = \text{sign}(f_2'(Z_1^*))$ the lemma follows directly. \square

403 The cases not covered by the lemma require a nonlinear analysis and will not be pursued
 404 further.

405 A coexistence steady state is a point (\hat{Z}_1, \hat{z}_2) satisfying $0 < f_1(\hat{Z}_1) = f_2(\hat{Z}_1) < 1$.

406 **Lemma 5** *If a coexistence point (\hat{Z}_1, \hat{z}_2) exists, then it is a saddle if $f_1'(\hat{Z}_1) < f_2'(\hat{Z}_1)$ and*
 407 *stable focus or a stable node if $f_1'(\hat{Z}_1) > f_2'(\hat{Z}_1)$ and $f_2'(\hat{Z}_1) < 0$.*

408 **PROOF.** The proof is straight forward computation by evaluating the trace and determinant
 409 of the Jacobian evaluated at the steady state. Negative determinant implies a saddle, while
 410 a positive determinant together with negative trace implies both eigenvalues have negative
 411 real part meaning that the steady state is a stable node or a stable focus.

$$\det(J((\hat{Z}_1, \hat{z}_2))) = -\beta_2 \hat{Z}_1 (1 - \hat{z}_2) F(\hat{Z}_1) \left(2\beta_4 \hat{Z}_1 F(\hat{Z}_1) - \frac{\beta_3 F'(\hat{Z}_1)}{F(\hat{Z}_1)} \right) \quad (39)$$

412 Then, notice that

$$f_1'(\hat{Z}_1) < f_2'(\hat{Z}_1) \Leftrightarrow 2\beta_4 \hat{Z}_1 F(\hat{Z}_1) - \frac{\beta_3 F'(\hat{Z}_1)}{F(\hat{Z}_1)} < 0 \quad (40)$$

413 proving that if (\hat{Z}_1, \hat{z}_2) exists, then it is a saddle if $f'_1(\hat{Z}_1) < f'_2(\hat{Z}_1)$.

414 Similarly, $\det\left(J\left((\hat{Z}_1, \hat{z}_2)\right)\right) > 0$ if $f'_1(\hat{Z}_1) > f'_2(\hat{Z}_1)$, hence eliminating saddle type fixed
415 point. As

$$tr\left((\hat{Z}_1, \hat{z}_2)\right) = \beta_3 \hat{Z}_1 \frac{F'(\hat{Z}_1)}{F(\hat{Z}_1)} + \beta_2 (1 - \hat{z}_2) F(\hat{Z}_1), \quad (41)$$

416 the trace is guaranteed to be negative if $F'(\hat{Z}_1) < 0$. Since

$$f'_2(Z_1) = \frac{\beta_3 F'(Z_1)}{-\beta_2 F(Z_1)^2}, \quad (42)$$

417 then a sufficient criterion for negative trace is $f'_2(\hat{Z}_1) < 0$ proving the second part of the
418 lemma. \square

419 A case not covered in the lemma is $f'_1(\hat{Z}_1) > f'_2(\hat{Z}_1) \wedge f'_2(\hat{Z}_1) > 0$. We can rule out
420 a saddle point, but the sign of the trace is not known. Perturbing a parameter such that
421 the trace changes sign while $f'_1(\hat{Z}_1) > f'_2(\hat{Z}_1)$ prior and after perturbation implies that
422 the real part of both eigenvalues shift sign at the same parameter value, suggesting a
423 Hopf-bifurcation. This is indeed possible to observe in simulations though this requires an
424 unrealistically large β_4 value, see figure 10.

425 **Lemma 6** *If $f_2(\tilde{Z}_1) > f_1(\bar{Z}_1)$ and $f_1(\bar{Z}_1) < 1$ then there exists a stable coexistence point*
426 *(\hat{Z}_1, \hat{z}_2) with $\bar{Z}_1 < \hat{Z}_1 < \tilde{Z}_1$ and $\hat{z}_2 < f_1(\bar{Z}_1)$ and there are no closed orbits enclosing*
427 *(\hat{Z}_1, \hat{z}_2) .*

428 **PROOF.** Recall that f_2 is strictly decreasing for $Z_1 > \tilde{Z}_1$ and $f_2(\tilde{Z}_1) = 0$ and f_1 is strictly
429 increasing. Hence, a unique intersection, $(\hat{Z}_1, f_1(\hat{Z}_1))$, between f_1 and f_2 exists for a
430 \hat{Z}_1 bounded above by \bar{Z}_1 and below by \tilde{Z}_1 . As $0 < f_1(Z_1) < 1$ for $0 < Z_1 < \bar{Z}_1$, then
431 $f_1(\hat{Z}_1) = \hat{z}_2 \in (0, 1)$. As $f'_2(\hat{Z}_1) < 0$ and $f'_1(\hat{Z}_1) > 0$ then (\hat{Z}_1, \hat{z}_2) is a stable steady state by
432 lemma 5. To show there can be no closed orbits encircling (\hat{Z}_1, \hat{z}_2) , consider figure 6. The
433 argument is based on showing existence of a continuum of invariant regions containing the
434 steady state point. Notice that for $\tilde{Z} < Z_1 \leq \bar{Z}$ then f_2 is monotone and hence f_2^{-1} is well
435 defined.

436 Any closed orbit encircling (\hat{Z}_1, \hat{z}_2) must have an intersection $P = (p_1, p_2)$ with $z_2 =$
437 $f_2(Z_1)$ for $Z_1 \in (\hat{Z}_1, \bar{Z}_1]$. Choosing a sufficiently small $\delta > 0$ we construct the box with
438 corners $(p_1 + \delta, p_2)$, $(p_1 + \delta, f_2(p_1 + \delta) + \delta)$, $(f_2^{-1}(f_2(p_1 + \delta) + \delta) - \delta, f_2(p_1 + \delta) + \delta)$,
439 $(f_2^{-1}(f_2(p_1 + \delta) + \delta) - \delta, p_2)$. Let the normal vector to the box be pointing outwards.
440 Consider the line segment of the box spanned by $(p_1 + \delta, p_2)$, $(p_1 + \delta, f_2(p_1 + \delta) + \delta)$. As
441 this line segment is to the right of the null cline of Z_1 , then $\dot{Z}_1 < 0$ everywhere on this line
442 segment. As the outward normal of the box is $(1, 0)$ everywhere on this line segment, then

443 $(\dot{Z}_1, \dot{z}_2) \cdot (1, 0) < 0$ showing the flow is pointing inwards to the box. By similar arguments,
 444 the flow is pointing inwards on the remaining three sides of the box, i.e the box is an
 445 invariant set. By existence and uniqueness at P the proposed closed orbit contains points
 446 both inside and outside the box region. However, any trajectory once in the box region
 447 cannot escape to reconnect at P from outside the box. Hence, there are no closed orbits
 448 encircling (\hat{Z}_1, \hat{z}_2) . \square

449 **Remark 3** If $f_2(0) > f_1(\bar{Z})$ and $f_1(\bar{Z}) < 1$ then lemma 6 is fulfilled and there is a
 450 unique coexistence point with positive Z_1 value. This out rules period solutions globally. A
 451 sufficient criterion for this is

$$\frac{1}{2}(2 - \beta_3) > \beta_4 \left(1 + \left(\frac{1 + \sqrt{1 + \beta_1}}{\beta_3} \right)^2 \right) \quad (43)$$

452 together with

$$1 > \beta_4 \left(1 + \left(\frac{1 + \sqrt{1 + \beta_1}}{\beta_3} \right)^2 \right). \quad (44)$$

453 If inequalities (43) and (44) are met then for sufficiently small $\epsilon > 0$ the set

$$T_3 = [\epsilon; M_1] \times [0; 1 - \epsilon] \quad (45)$$

454 is invariant to the flow, and the only steady state in T_3 is the coexistence steady state. By
 455 the Poincaré Bendixon Theorem this point is then attracting all trajectories in T_3 i.e. the
 456 following lemma is proved

457 **Lemma 7** For $\beta_2 < 0, \beta_3 < 2, \beta_4 > 0, \frac{1}{2}(2 - \beta_3) > \beta_4 \left(1 + \left(\frac{1 + \sqrt{1 + \beta_1}}{\beta_3} \right)^2 \right), 1 > \beta_4 \left(1 + \left(\frac{1 + \sqrt{1 + \beta_1}}{\beta_3} \right)^2 \right)$
 458 a unique, positive, coexistence steady state of equation (20) exists which attracts all trajec-
 459 tories with $Z_1(0) > 0, z_2(0) < 1$.

460 **Remark 4** If there is one steady state satisfying lemma 6, and any other coexistence steady
 461 state with positive Z_1 value is a saddle, then there are no closed orbits. This is due to index
 462 theory [47] that disallows a closed orbit solely enclosing one or more saddles.

463 Considering again the necessary condition for a coexistence point $f_1(Z_1) = f_2(Z_1)$
 464 which implies

$$\sqrt{1 + \beta_1 Z_1} (1 - \beta_4 (1 + Z_1^2)) = (\beta_3 + \beta_4) (1 + Z_1^2) - 1. \quad (46)$$

Squaring this expression and collection terms of same order, the Z_1 - value at the coexis-
 tence point must satisfy a fifth order polynomial

$$\begin{aligned} 0 = & -\alpha_2 \alpha_5^2 Z_1^5 + (\alpha_4^2 + 2\alpha_4 \alpha_5) Z_1^4 + (-2\alpha_2 \alpha_5^2 + 2\alpha_2 \alpha_5) Z_1^3 \\ & + (2\alpha_4^2 + 4\alpha_4 \alpha_5 - 2\alpha_4) Z_1^2 + (-\alpha_2 \alpha_5^2 + 2\alpha_2 \alpha_5 - \alpha_2) Z_1 + \alpha_4^2 + 2\alpha_4 \alpha_5 - 2\alpha_4, \end{aligned} \quad (47)$$

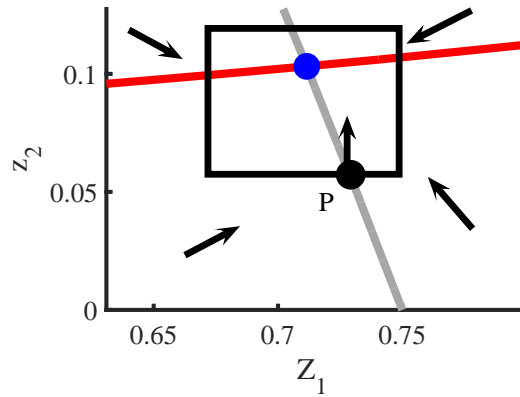


Figure 6: Illustration of no limit cycle when the conditions of lemma 6 are fulfilled. The red curve is the null cline of \dot{z}_2 , grey curve is the null cline of \dot{Z}_1 . Any limit cycle must enclose a critical point and for the parameter constraints considered, there is exactly one coexistence steady state (blue dot). Therefore, any limit cycle must intersect the null cline of Z_1 , denote such a point P . Construct a rectangular box as shown. At P the flow is along the z_2 - axis hence pointing into the box. As the existence and uniqueness theorem applies, the trajectory through P consists of points both inside and outside of the box. However, the box is a trapping region as seen by inspection of the null clines and that \dot{Z}_1 and \dot{z}_2 are continuous in Z_1 and z_2 . Therefore, the trajectory through P entering the box cannot escape it to reconnect with P from outside the box. Hence, there can be no limit cycle through P , and hence no limit cycle at all.

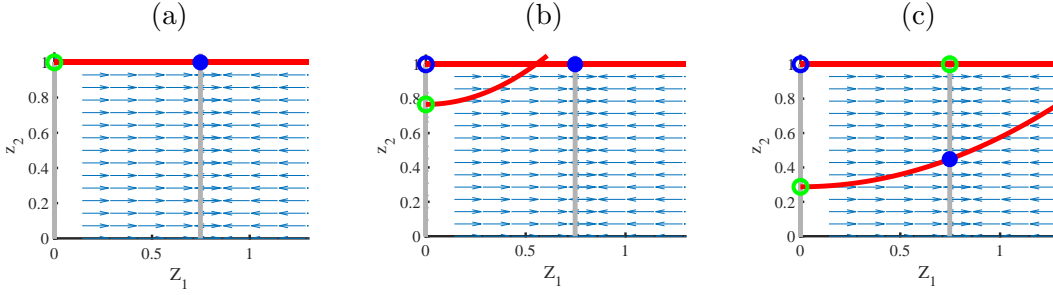


Figure 7: Phase space for $\beta_2 < 0$ small with increasing numerical value, all other parameters at default values. In (a) $\beta_2 = -2 \cdot 10^{-5}$, in (b) $\beta_2 = -3 \cdot 10^{-5}$, and in (c) $\beta_2 = -8 \cdot 10^{-5}$. As the two null clines cross, a stable coexistence steady state is created, changing the stability of the cancer steady state from stable to unstable. For increasing $|\beta_2|$ the stable equilibrium has decreasing z_2 value. The dynamics is a fast attraction to the stable Z_1 null cline and the a slower attraction to the stable coexistence steady state / cancer steady state. As equation (47) is independent of β_2 , the inner coexistence point (when it exists) moves parallel to the z_2 - axis as β_2 is varied.

	(a)	(b)	(c)	(d)	(e)	(f)	(g)	(h)
β_1	5	4	4	2	5	2	2	5
β_2	-.2793	-.2793	-.1676	-.1676	-.2793	-.1676	-.1676	-.1816
β_3	1.3	1.95	1.95	1.2	1.3	1.74	1.8	1.73
β_4	.3313	.1988	.2916	.106	.1	.0133	.0133	.8469

Table 3: Parameter values for figure 8, (a)-(h)

465 with the constraint that equation (46) must be valid. Then, the z_2 value at the coexistence
466 point can be computed from equation (35). Notice that equation (47) is independent of β_2
467 while equation (35) is not. Therefore, perturbing β_2 the coexistence point moves parallel
468 to the z_2 axis, see figure 7. Hence, increasing the self renewal of CSC compared to HSC
469 increase the allele burden but not the total blood cell count in this case. The polynomial
470 formulation of the steady state is easily implemented in e.g. Matlab for numerical
471 implementation.

472 Possible phase planes for $-1 < \beta_2 < 0, \beta_4 > 0, 0 < \beta_3 < 2$ are shown in figure 8.
473 The different cases are found by investigating the existence and order of $z_2 = f_1(Z_1)$ and
474 $z_2 = f_2(Z_1)$ crossing each other and the boundaries. We have found no more than two
475 coexistence steady states with positive Z_1 value, for a given parameter set of parameter
476 values.

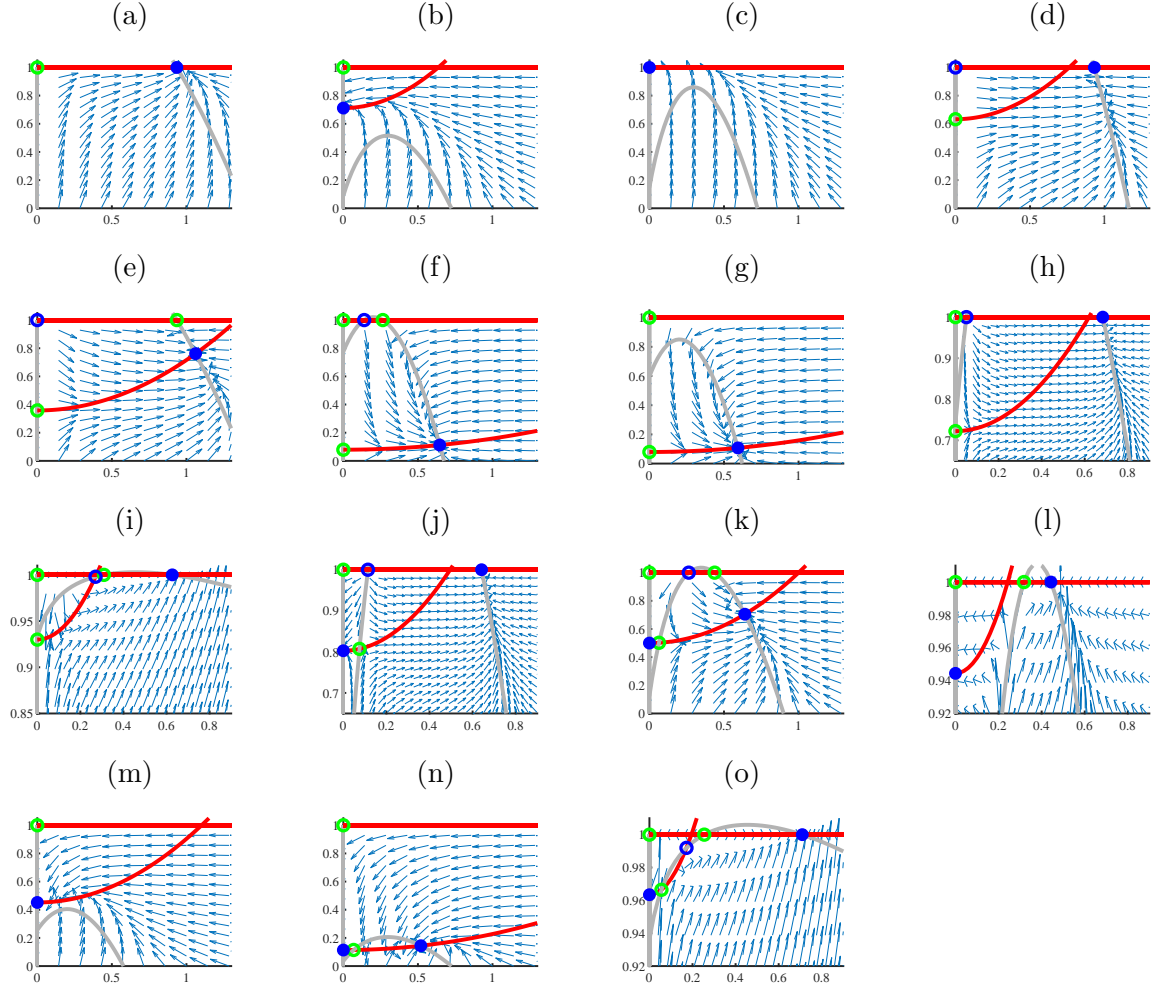


Figure 8: Phase plane, (Z_1, z_2) , for $-1 < \beta_2 < 0$, $\beta_4 > 0$. Corresponding parameter values are listed in table 3 and 4. In all cases except (i) and (o), there can be no period orbits, hence the steady states are the only possible attractors. Unhealthy attractors are located on the lines $Z_1 = 0$ and $z_2 = 1$, while a coexistence steady state with positive Z_1 value may be unhealthy or healthy, for example (f), (g), (n) may be considered healthy conditions for most initial conditions.

	(i)	(j)	(k)	(l)	(m)	(n)	(o)
β_1	20	6	6	8	2	4	20
β_2	-.9107	-.1536	-.2000	-.2933	-.2933	-.6984	-.9079
β_3	0.3	1.92	1.95	1.85	1.85	1.95	.3
β_4	.8469	.1233	.1	.2770	.1325	.0795	.8747

Table 4: Parameter values for figure 8, (i)-(o)

477 **2.4.8 The case $\beta_2 = -1, \beta_4 > 0$**

478 This case is similar to $0 > \beta_2 > -1$ except there can be no cancer steady states and hence
479 will not be elaborated further. The possible topologies are shown in figure 9.

480 **3 Discussion**

481 A two dimensional model is presented to investigate the dynamics of cancer and hematopoi-
482 etic stem cells and mature cells, immune system activity, and clearing of dead cells, in-
483 cluding a nonlinear niche feedback with competition between the two stem cell types. In
484 the model the self renewal rates for HSC and CSC are allowed to differ while some other
485 parameters being assumed equal for the HSC and CSC dynamics. For a wide range of
486 parameter values, analytical insight in the global dynamics is obtained revealing that the
487 competition at stem cell level, β_2 , is crucial for whether hematopoiesis is maintained or
488 MPN dominates. In particular, $\beta_2 > 0$ is a signature of cancer growth out competing
489 healthy hematopoietic cells, while $\beta_2 < 0$ is needed for stable hematopoiesis or a sustained,
490 low cancer burden.

491 **3.1 Elevated *JAK2* in patients without MPN diagnosis**

492 Blood samples from non MPN diagnosed patients have been analyzed by Xu et al. [73]
493 who found that about 1% of the 3935 investigated subjects were *JAK2* positive, with 70%
494 of these having low allele burdens i.e. less than 5%. A general population study found that
495 0.2% of the population harbours the *JAK2* mutation [50]. In a large Swedish study [29],
496 the number of patients with MPN is found as 3035 during the years 2001 to 2008. With a
497 population size of 9 millions this implies a prevalence of 0.03%.

498 How can the role of *JAK2* mutation as a driver for cancer development for MPN patients
499 be consistent with many carrying the *JAK2* mutation do not have an MPN diagnosis?
500 One explanation could of course be, that a large number of subjects were in an early, yet
501 undiagnosed state of MPNs.

502 Traulsen et al. [67] suggest another reason, namely that the *JAK2* mutation found in
503 the study of [73] is not occurring at the stem cell level but further down the proliferation
504 chain hence not affecting hematopoiesis so severely. This would imply that after some

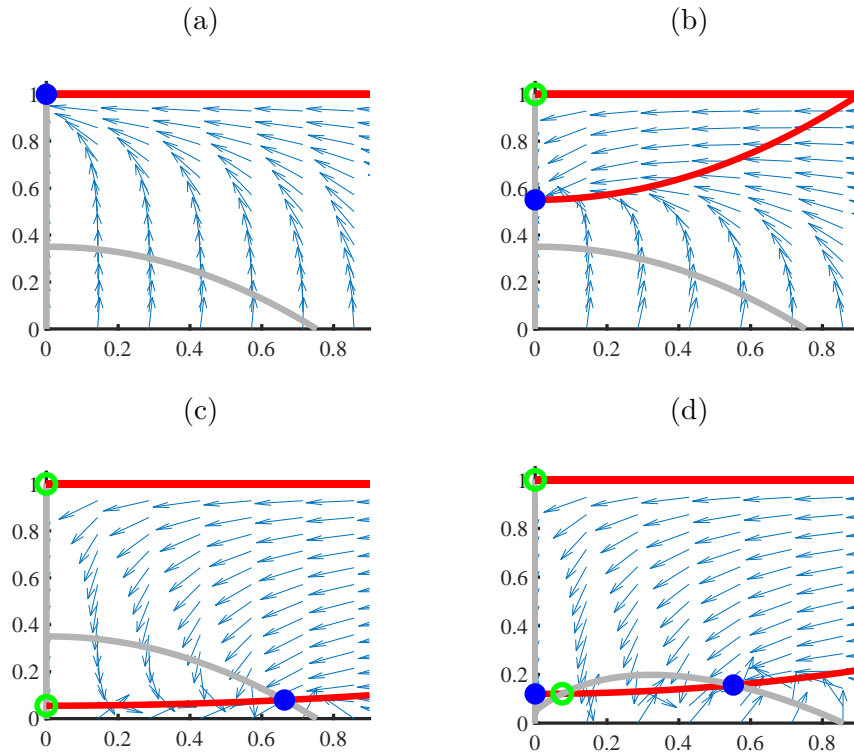


Figure 9: Phase space for $\beta_2 = -1$. (a) and (b) are unhealthy conditions while (c) and (d) are healthy for most initial conditions.

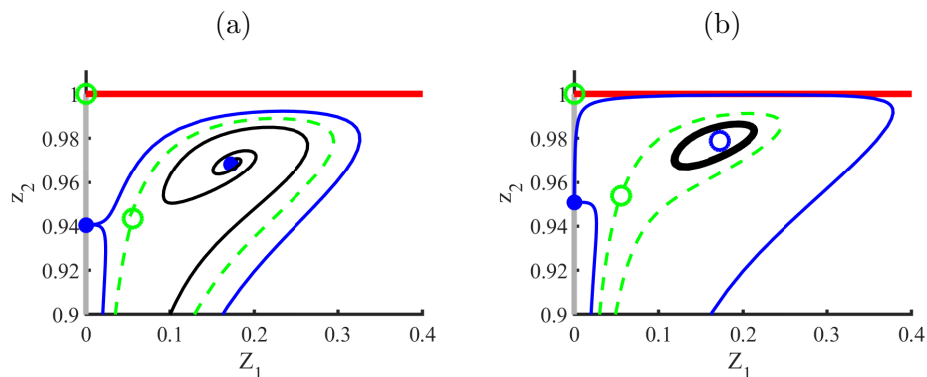


Figure 10: In (a) there are two stable steady states and two saddles. Selected trajectories are shown in green, blue and black curves. Parameter values are $\beta_1 = 20, \beta_2 = -.93, \beta_3 = .3, \beta_4 = .8747$. In (b) $\beta_2 = -.92$ with the remaining parameter values being the same as in (a). A Hopf- bifurcation has occurred for some $\beta_2 \in (-.92; -.93)$ such that a stable coexistence steady state has turned unstable and a stable limit cycle has appeared.

505 time, the *JAK2* positive cells are depleted. However, a small, stable *JAK2* fraction can
 506 be maintained for years [18]. Our analysis suggests an alternative answer; the non MPN
 507 diagnosed subjects are characterized by parameter values rendering a stable, coexistence
 508 point with low allele burden corresponding to figure 8(f), (g), (n). Alternatively, the MPN
 509 fraction of cells may be slowly increasing corresponding to HSC and CSC selfrenewal being
 510 of comparable size. This may be more feasible than multiple *JAK2* mutations in the
 511 same individual [42]. Another interesting explanation is the '*active immune window*' where
 512 malignant cells need to reach a critical level before the immune system is activated to keep
 513 a low disease level. This has proven a fruitful explanation for describing clinical data of
 514 patients with chronic myeloid leukemia [7].

515 3.2 Intervention strategies

516 From the previous analysis it is clear that the sign of β_2 is important for treatment outcome.
 517 Intervention at stem cell level is important to ensure cure or minimal residual disease
 518 which is relevant also for chronic myeloid leukemia [10]. In figure 11 a model simulation
 519 with default parameter values is shown along with median data of two sets of patients
 520 with polycythemia vera treated with pegylated interferon- α -2a [53], [30]. Altering β_2
 521 by decreasing r_y and increasing r_x corresponds to a mechanism of the drug where the
 522 malignant clone is targeted [53][31] and HSC are activated [17]. Only the initial conditions
 523 vary, corresponding to a different initial allele burden for each group of study. Hence,
 524 by altering β_2 to the value -0.9 , two clinical data sets can be reproduced using a single
 525 parameter set in the model.

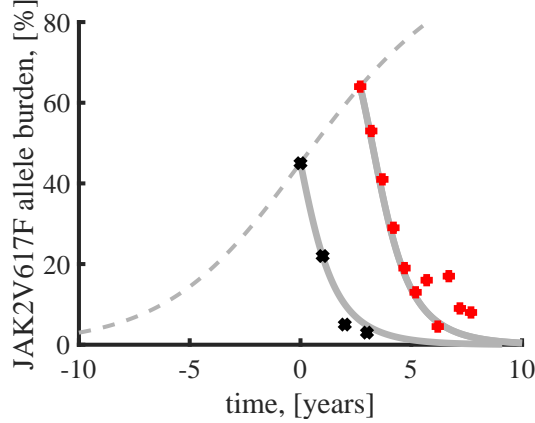


Figure 11: Grey stipulated curve is cancer growth using the default parameter values in the simple model shifted in time such that the *JAK2* allele burden is 45% at $t = 0$. Dots are median values from two independent clinical studies of patients with polycythemia vera treated with pegylated interferon- α -2a. Red dots are from [53] (43 patients), black dots are from [30] (40 patients). Full grey curves are output of the simple model, with $\beta_2 = -0.9$, which is obtained by a doubling in r_x as interferon increases stem cell activity [17] and a reduction in r_y . Remaining parameters set to default values. The only difference between the two grey curves are the initial conditions. Hence, the simple model with a unique set of parameter values can reproduce several clinical reports on PV patients with the explained effect being related to increased HSC function compared to CSC during treatment.

526 The phase plane dynamics with β_2 having small, negative values are shown in figure
 527 7 showing how a stable cancer steady state bifurcates to a stable coexistence steady state
 528 when perturbing β_2 . In figure 12, two treatment scenarios are shown based on changing β_2
 529 from positive to negative values. Starting treatment at a high allele burden can ultimately
 530 lead to reversal to a healthy, hematopoietic steady state or a coexistence steady state with
 531 low allele burden. An effective drug (high dose) may have the negative impact that the
 532 total number of white blood cells have critically low values in the transition from a high
 533 allele burden to a healthy state as can be seen by considering the trajectories in figure 12.
 534 This suggests that maintaining a low dose or slowly increasing dose during treatment may
 535 be important, or that treatment should also address other parameters.

536 Intervention at an early cancer stage is preferred for several reasons for example reduc-
 537 ing the risk of thrombosis or hemorrhage. Our phase plane analysis suggests further that
 538 an early intervention can lead to a coexistence steady state with low tumor load while late
 539 intervention may lead to out competition of healthy cells even though the self renewal of
 540 HSC is larger than that of CSC. This may occur when there are three coexistence steady

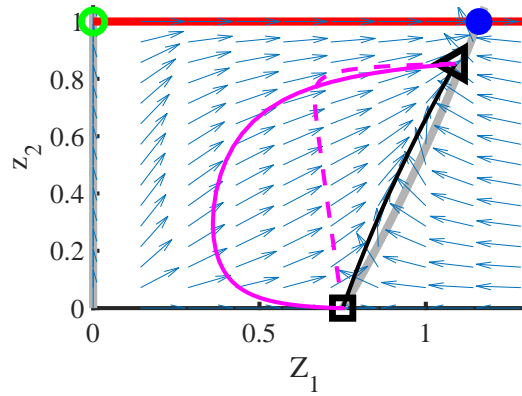


Figure 12: Phase space with default parameter values where the full blown MPN cancer is the stable steady state. A typical trajectory (black curve) is shown with initial condition in the black square. A successful treatment must change the sign of β_2 from positive to negative. At the triangle, two different treatments are initiated (magenta), for the full curves $\beta_2 = -0.9$ and for the dashed $\beta_2 = -0.1$. The temporary, small value of Z_1 at the full, magenta curve suggests that an effective treatment may reduce the number of white blood cells too severely. However, a more gradual change of β_2 corresponding to a slowly increasing dose of an effective drug does not have the same shortcoming.

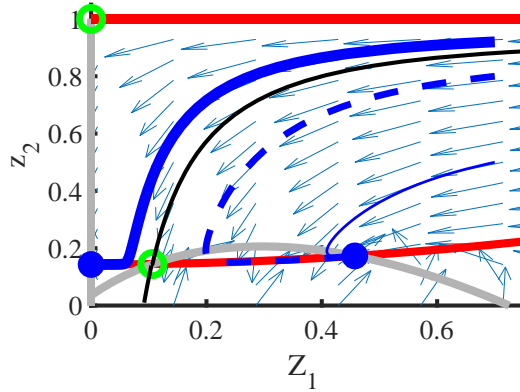


Figure 13: Possible phase plane for $\beta_2 < 0, \beta_4 > 0$. Blue curves are specific trajectories. Black curves are the stable manifolds of the saddle point (green circle) dividing the phase space in two basins of attraction. In the right region the stable, coexistence point is a relatively healthy state while the left region implies extinction of healthy cells for any initial condition. The case showed here may be a result of intervention with $\beta_2 > 0$ prior to intervention and $\beta_2 < 0$ after intervention. Early intervention leads to an initial condition in the lower right part of the phase space which corresponds to a non expanding malignant cell count i.e. a relatively healthy condition. The thick blue curve shows that the same intervention at large, initial malignant cell counts can lead to eradication of healthy cells.

541 states, for initial conditions with large allele burdens are in the basin of attraction of the
 542 stable steady state causing extinction of healthy cells - see figure 13. Furthermore, for ini-
 543 tial conditions in the basin of attraction of the relatively healthy coexistence steady state,
 544 a high initial allele burden implies a transient with a low Z_1 value compared to the steady
 545 state. Hence, late treatment start may imply more serious adverse events which advocates
 546 for early treatment. The separatrix (black curve) provides a threshold for initial condi-
 547 tions that will maintain homeostasis versus eradicate healthy cells. A similar approach has
 548 proven useful for dynamics of Hepatitis C Virus and immune suppression [35].

549 3.3 Comparison of the simple and full model

550 The simple model is a good representation of the full model for cancer progression. An
551 important reason for this is the assumption that cancer initiation is a perturbation to
552 a hematopoietic steady state i.e. initially $y'_0 = y'_1 = a' = s' = 0$ which implies that
553 no transients are observed for the trajectories of the full model to be close to the simple
554 model. Initiating a treatment may be interpreted as a fast change in one or more parameter
555 values. In figure 14 the simple and full model are evolved with default parameter values
556 until an allele burden of 50% is obtained. Then, a parameter value is abruptly changed,
557 and the resulting trajectories of stem cells and mature blood cells are shown for the full
558 and simple model. The simple model is a good approximation to the full model when
559 altering a stem cell parameter value such as r_x or r_y as seen in figure 14(a) which supports
560 the use of the simple model in figure 11. Changing a parameter value of the mature cells
561 such as d_{x1} lead to a discontinuity in the simple model and a fast transient in the full
562 model, hence for a short time the full model and the reduced model do not match - see
563 14(b). This discontinuity is expected in the simple model from equation (3c); a jump in
564 d_{x1} leads to a jump in x_1 . Hence, for treatments mainly affecting mature cells, a fast
565 transient between the full and the reduced model may be observed. The full model and the
566 simple model have exactly the same steady states. However, the stability steady states in
567 a quasi steady state model and a full model may differ. In figure 15 a bifurcation diagram
568 is shown for the reduced model model by computing steady states and their stability at
569 500 times 250 grid points. Likewise, the corresponding steady state of the full model can
570 be investigated by fixing all full model parameters at default values except r_m, r_y, e_s and
571 r_s that can be computed from the values of $\beta_1, \beta_2, \beta_3$ and β_4 by inverting equation (21).
572 Then, the stability of the full model is assessed by the dominant eigenvalue of the six by
573 six dimensional Jacobian. The stability of the full model and simple model are found to
574 be identical everywhere.

575 3.4 Early MPN phase

576 One hit mutation

577 Assuming little change in Z_1 in the early cancer phase, we may derive expressions for
578 cancer growth for a one hit mutation, i.e. $\beta_4 = 0$. In that case

$$\dot{z}_2 = k_1 \beta_2 (1 - z_2) z_2, \quad (48)$$

579 with $k_1 = \frac{1 + \sqrt{1 + \beta_1 \bar{Z}_1}}{1 + \bar{Z}_1^2}$ and with the initial condition being a positive, small allele burden, z_{20}
580 at time equal to zero. This equation may be solved providing the well known expression
581 for logistic growth. Such an expression is well known in cancer descriptions. However,
582 the approach here with the logistic growth as an asymptotic case of a more elaborate
583 model allows for inferring mechanisms to the parameters of the one dimensional model

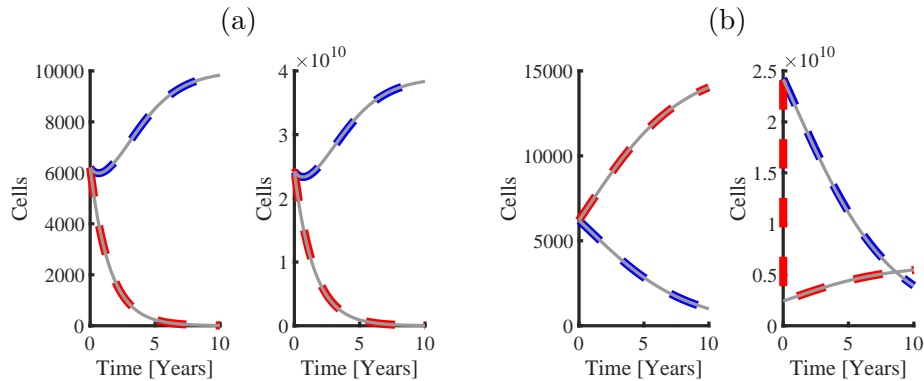


Figure 14: Initial conditions correspond to integrating the full or simple model with default parameter values until equal amounts of hematopoietic and cancer stem cells. Then, an abrupt change in a parameter value is applied, representing a potential treatment. In (a) β_2 is changed to -0.9 by reducing r_y and doubling r_x which correspond to the suggested effect of pegylated interferon- α -2a in figure 11. Left panel is stem cell numbers, right panel is mature cell numbers. Blue curves are hematopoietic cells, red are blood cancer cells. Grey curves are the corresponding trajectories from the simple model. For an abrupt change in stem cell parameters, the simple model, (3) remains a good approximation to the full model (1). In (b) the value of d_{y1} is increased by a factor 10 with the remaining parameters at default value. Here, the mature cancer cell count drops immediately in the simple model while the full model has a fast transient before good agreement again is observed between the full model and the two dimensional model. Though an increased death rate of mature, cancer cells implies an immediate reduction of mature cancer cells, the mature hematopoietic cells are not restored by this intervention and in the long run, the mature cancer cells again dominates the mature hematopoietic cells i.e. this intervention does not provide a cure.

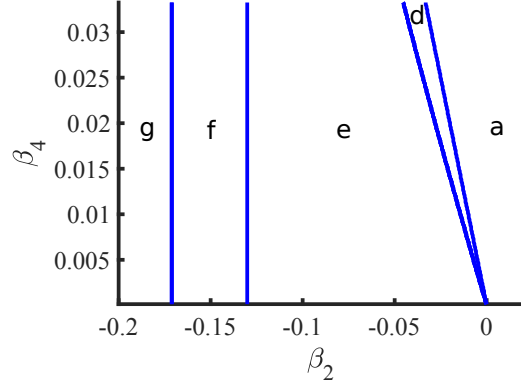


Figure 15: Bifurcation diagram, with $\beta_1 = 2$, $\beta_3 = 1.74$ and varying β_2 and β_4 . The letters on the figure correspond to the topologies in figure 8, hence showing possible transitions between the topologies as parameters are perturbed. In regions g, f, e the stable steady state is a coexistence steady state, while in regions d and a a cancer steady state is the only stable steady state.

584 equation (48). Thus, in the early cancer phase, if the disease is diagnosed and treatment is
 585 conducted, which change the sign of β_2 from positive to negative with new value denoted
 586 $\hat{\beta}_2$, then, disease progression is changed from logistic growth to logistic decay. However,
 587 the dose-response relation may be unknown. Comparing the growth curve at allele burden,
 588 z_2 before treatment to allele burden \hat{z}_2 after treatment using the lab time t we observe

$$\frac{z_2'}{\hat{z}_2'} = \frac{\beta_2 (1 - z_2) z_2}{\hat{\beta}_2 (1 - \hat{z}_2) \hat{z}_2}. \quad (49)$$

589 This means that the change in stem cell parameters, $\frac{\beta_2}{\hat{\beta}_2}$ can be directly computed from
 590 considering the slope of allele burden of mature cells prior to and after treatment without
 591 use of sophisticated parameter estimation techniques. In this way, mathematical modelling
 592 and reasoning give a window to investigate the hardly accessible stem cell dynamics by
 593 mechanistic modelling and measurements of the mature cells.

594 Solving (48) with a change of β_2 value to another value $\hat{\beta}_2$ at time $\tau = T$ gives

$$z_2(\tau) = \frac{z_{20} e^{\beta_2 k_1 \tau}}{z_{20} (e^{\beta_2 k_1 \tau} - 1) + 1}, \quad \text{for } 0 \leq \tau \leq T \quad (50a)$$

$$\hat{z}_2(\tau) = \frac{z_2(T) e^{\hat{\beta}_2 k_1 (\tau - T)}}{z_2(T) (e^{\hat{\beta}_2 k_1 (\tau - T)} - 1) + 1}, \quad \text{for } \tau > T \quad (50b)$$

595

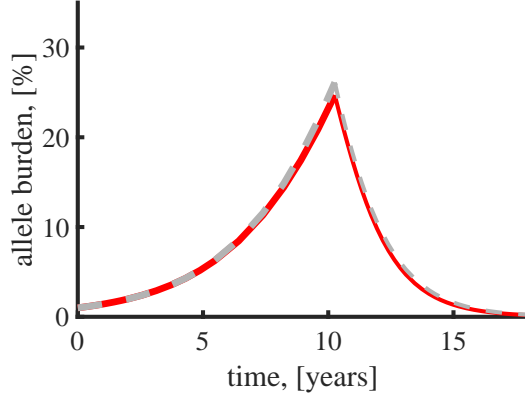


Figure 16: Red, thick curve is allele burden growth using the simple, reduced model with default parameters. At year 10, a treatment intervention changes the β_2 value to -0.9 showed by the thin red, solid line. Grey curves are the corresponding analytic approximation given by equation (50) with $z_2(0) = 0.01$ corresponding to the sensitivity of the best assays.

596 A comparison of this formula to the simple, reduced model is seen in figure 16 providing
 597 a good approximation within the measurable, low allele burden regime.

598 3.5 Role of exogenous inflammation stimuli

We reformulate equation 50 in terms of the original parameters

$$z_2(t) = \frac{z_{20}e^{\gamma t}}{z_{20}(e^{\gamma t} - 1) + 1}, \quad \text{for } 0 \leq t \leq \hat{T} \quad (51a)$$

$$z_2(t) = \frac{z_2(\hat{T})e^{\hat{\gamma}(t-\hat{T})}}{z_2(\hat{T})(e^{\hat{\gamma}(t-\hat{T})} - 1) + 1}, \quad \text{for } t > \hat{T} \quad (51b)$$

599 with

$$\gamma = \frac{r_y - r_x}{2e_s(1 + \bar{Z}_1^2)} \left(I + \sqrt{I^2 + \left(4 \frac{e_s r_s}{c_{xx} e_a} (a_x A_x + d_{x0}) \right) \bar{Z}_1} \right). \quad (52)$$

600 This implies $|\gamma|$ increases with I , i.e. disease progression is accelerated for a large endoge-
 601 nous inflammatory stimuli, when $r_y > r_x$. Surprisingly, in case an intervention happens,
 602 such that $r_y > r_x$ prior to treatment but $r_x > r_y$ after treatment, then inflammation acts
 603 as a disease driver prior to treatment but after treatment inflammation acts like a health
 604 promoter. Similarly, one may predict the behaviour of perturbing the original parameters
 605 $e_s, r_s, c_{xx}, e_a, a_x, A_x, d_{x0}$.

606 4 Appendix

607 Derivation of the simple Cancitis model

Model is (1) written here again for convenience

$$x'_0 = (r_x \phi_x s - d_{x0} - a_x) x_0 - r_m s x_0 \quad (53a)$$

$$x'_1 = a_x A_x x_0 - d_{x1} x_1 \quad (53b)$$

$$y'_0 = (r_y \phi_y s - d_{y0} - a_y) y_0 + r_m s x_0 \quad (53c)$$

$$y'_1 = a_y A_y y_0 - d_{y1} y_1 \quad (53d)$$

$$a' = d_{x0} x_0 + d_{y0} y_0 + d_{x1} x_1 + d_{y1} y_1 - e_a a s \quad (53e)$$

$$s' = r_s a - e_s s + I(t) \quad (53f)$$

$$\phi_x = \phi_x(x_0, y_0) = \frac{1}{1 + (c_{xx} x_0 + c_{xy} y_0)^2} \quad (53g)$$

$$\phi_y = \phi_y(x_0, y_0) = \frac{1}{1 + (c_{yx} x_0 + c_{yy} y_0)^2} \quad (53h)$$

608 These equations are subject to a quasi steady state assumption of all compartments except
609 the stem cells

$$x'_1 = y'_1 = a' = s' = 0, \quad (54)$$

610 and with constant I . From $x'_1 = 0$, x_1 is easily expressed as

$$x_1 = \frac{a_x A_x}{d_{x1}} x_0, \quad (55)$$

611 and similarly $y'_1 = 0$ implies

$$y_1 = \frac{a_y A_y}{d_{y1}} y_0. \quad (56)$$

612 From $s' = 0$ we get

$$a = \frac{e_s}{r_s} s - \frac{I}{r_s} \quad (57)$$

613 Inserting this in equation (53e) with $a' = 0$ we arrive at

$$0 = d_{x0} x_0 + d_{y0} y_0 + d_{x1} x_1 + d_{y1} y_1 - e_a s \left(\frac{e_s}{r_s} s - \frac{I}{r_s} \right) \quad (58)$$

614 which may be considered a second order polynomial in s . Solving for the roots we get

$$s_{\pm} = \frac{I}{2e_s} \pm \sqrt{\left(\frac{I}{2e_s} \right)^2 + \frac{r_s}{e_s e_a} (d_{x0} x_0 + d_{y0} y_0 + d_{x1} x_1 + d_{y1} y_1)} \quad (59)$$

615 As we are only interested in non negative s values, only $s = s_+$ is kept and equation (55)
 616 and equation (56) are inserted to give

$$s = \frac{I}{2e_s} + \sqrt{\left(\frac{I}{2e_s}\right)^2 + \frac{r_s(a_x A_x + d_{x0})}{e_a e_s} \left(x_0 + \frac{a_y A_y + d_{y0}}{a_x A_x + d_{x0}} y_0\right)} \quad (60)$$

617 Inserting this expression for s in equation (57) provides a as a function of x_0 and y_0

$$a = -\frac{I}{2r_s} + \frac{e_s}{r_s} \sqrt{\left(\frac{I}{2e_s}\right)^2 + \frac{r_s(a_x A_x + d_{x0})}{e_a e_s} \left(x_0 + \frac{a_y A_y + d_{y0}}{a_x A_x + d_{x0}} y_0\right)} \quad (61)$$

618 Differential equations (53a) and (53c) together with the algebraic equations (55), (56), (59)
 619 and (61) constitute the simple cancer model.

620 References

- 621 [1] M. ANDERSEN, Z. SAJID, R. K. PEDERSEN, J. GUDMAND-HØEYER, C. ELLERVIK,
 622 V. SKOV, L. KJÆR, N. PALLISGAARD, T. A. KRUSE, M. THOMASSEN,
 623 J. TROELSEN, H. C. HASSELBALCH, AND J. T. OTTESEN, *Mathematical modelling as*
 624 *a proof of concept for MPNs as a human inflammation model for cancer development*,
 625 PLoS ONE, 12 (2017), pp. 1–18.
- 626 [2] P. ASHCROFT, M. G. MANZ, AND S. BONHOEFFER, *Clonal dominance and trans-*
 627 *plantation dynamics in hematopoietic stem cell compartments*, PLoS Computational
 628 Biology, 13 (2017), pp. 1–20.
- 629 [3] L. BEREZANSKY, E. BRAVERMAN, AND L. IDELS, *Mackey-Glass model of*
 630 *hematopoiesis with monotone feedback revisited*, Applied Mathematics and Compu-
 631 tation, 219 (2013), pp. 4892–4907.
- 632 [4] A. BESSE, G. D. CLAPP, S. BERNARD, F. E. NICOLINI, D. LEVY, AND T. LEP-
 633 OUTRE, *Stability Analysis of a Model of Interaction Between the Immune System and*
 634 *Cancer Cells in Chronic Myelogenous Leukemia*, Bulletin of Mathematical Biology, 80
 635 (2018), pp. 1084–1110.
- 636 [5] M. A. BÖTTCHER, D. DINGLI, B. WERNER, AND A. TRAUlsen, *Replicative cellular*
 637 *age distributions in compartmentalized tissues.*, Journal of the Royal Society, Interface,
 638 15 (2018-08-01).
- 639 [6] S. N. CATLIN, L. BUSQUE, R. E. GALE, P. GUTTORP, AND J. L. ABKOWITZ,
 640 *The replication rate of human hematopoietic stem cells in vivo*, Blood, 117 (2011),
 641 pp. 4460–4466.

- 642 [7] G. D. CLAPP, T. LEPOUTRE, R. EL CHEIKH, S. BERNARD, J. RUBY,
643 H. LABUSSIÈRE-WALLET, F. E. NICOLINI, AND D. LEVY, *Implication of the autolo-*
644 *gous immune system in bcr-abl transcript variations in chronic myelogenous leukemia*
645 *patients treated with imatinib*, *Cancer Research*, 75 (2015), pp. 4053–4062.
- 646 [8] B. M. CRAVER, K. EL ALAOU, R. M. SCHERBER, AND A. G. FLEISCHMAN, *The*
647 *critical role of inflammation in the pathogenesis and progression of myeloid malignan-*
648 *cies.*, *Cancers*, 10 (2018-04-03).
- 649 [9] C. DESTERKE, C. MARTINAUD, N. RUZEHAJI, AND M. C. LE BOUSSE-KERDILÉS,
650 *Inflammation as a keystone of bone marrow stroma alterations in primary myelofibro-*
651 *sis*, *Mediators of Inflammation*, 2015 (2015), p. 16.
- 652 [10] D. DINGLI AND F. MICHOR, *Successful therapy must eradicate cancer stem cells*, *Stem*
653 *Cells*, 24 (2006), pp. 2603–2610.
- 654 [11] D. DINGLI AND J. M. PACHECO, *Modeling the architecture and dynamics of*
655 *hematopoiesis*, *Wiley Interdisciplinary Reviews: Systems Biology and Medicine*, 2
656 (2010), pp. 235–244.
- 657 [12] ———, *Stochastic dynamics and the evolution of mutations in stem cells*, *BMC Biology*,
658 9 (2011), pp. 1–7.
- 659 [13] D. DINGLI, A. TRAUlsen, AND F. MICHOR, *(A) Symmetric Stem Cell Replication*
660 *and Cancer*, *PLoS Computational Biology*, 3 (2007), pp. 30083–30083.
- 661 [14] M. DOUMIC, A. MARCINIAK-CZOCHRA, B. PERTHAME, AND J. ZUBELLI, *A struc-*
662 *tured population model of cell differentiation*, *SIAM J. Appl. Math.*, 71 (2011),
663 pp. 1918–1940.
- 664 [15] A. ELADDADI, P. KIM, AND D. MALLET, *Mathematical Models of Tumor- Immune*
665 *System Dynamics*, Springer New York, (2016).
- 666 [16] H. ENDERLING, *Cancer stem cells: small subpopulation or evolving fraction?*, *Inte-*
667 *grative biology*, 7 (2014), pp. 14–23.
- 668 [17] M. A. G. ESSERS, S. OFFNER, W. E. BLANCO-BOSE, Z. WAIBLER, U. KALINKE,
669 M. A. DUCHOSAL, AND A. TRUMPP, *IFN alpha activates dormant haematopoietic*
670 *stem cells in vivo*, *Nature*, 458 (2009), pp. 904–8.
- 671 [18] R. E. GALE, A. J. R. ALLEN, M. J. NASH, AND D. C. LINCH, *Long-term serial*
672 *analysis of X-chromosome inactivation patterns and JAK2 V617F mutant levels in*
673 *patients with essential thrombocythemia show that minor mutant-positive clones can*
674 *remain stable for many years*, *Blood*, 109 (2007-02-01), pp. 1241,1243.

- 675 [19] S. GENTRY AND T. JACKSON, *A mathematical model of cancer stem cell driven tumor*
676 *initiation: Implications of niche size and loss of homeostatic regulatory mechanisms*,
677 PLoS ONE, 8 (2013), p. e71128.
- 678 [20] P. GETTO, A. MARCINIAK-CZOCHRA, Y. NAKATA, AND M. D.M. VIVANCO, *Global*
679 *dynamics of two-compartment models for cell production systems with regulatory mech-*
680 *anisms*, Mathematical Biosciences, 245 (2013), pp. 258–268.
- 681 [21] H. HAENO, R. L. LEVINE, D. G. GILLILAND, AND F. MICHOR, *A progenitor cell*
682 *origin of myeloid malignancies*, Proceedings of the National Academy of Sciences,
683 (2009).
- 684 [22] H. C. HASSELBALCH, *Perspectives on chronic inflammation in essential thrombo-*
685 *cythemia, polycythemia vera, and myelofibrosis: is chronic inflammation a trigger and*
686 *driver of clonal evolution and development of accelerated atherosclerosis and second*
687 *cancer?*, Blood, 119 (2012), pp. 3219–3225.
- 688 [23] ———, *Chronic inflammation as a promotor of mutagenesis in essential thrombo-*
689 *cythemia, polycythemia vera and myelofibrosis. a human inflammation model for can-*
690 *cer development?*, Leukemia Research, 37 (2013), pp. 214–220.
- 691 [24] ———, *A role of nf-e2 in chronic inflammation and clonal evolution in essential throm-*
692 *bocytthemia, polycythemia vera and myelofibrosis?*, Leukemia Research, 38(2) (2014),
693 pp. 263–266.
- 694 [25] H. C. HASSELBALCH, *Smoking as a contributing factor for development of poly-*
695 *cythemia vera and related neoplasms*, Leukemia Research, 39 (2015-11), pp. 1137,1145.
- 696 [26] H. C. HASSELBALCH AND M. BJØRN, *MPNs as Inflammatory Diseases: The Evi-*
697 *dence, Consequences, and Perspectives*, Mediators of Inflammation, (2015), pp. 1–16.
- 698 [27] S. HERMOUET, E. BIGOT-CORBEL, AND B. GARDIE, *Pathogenesis of myeloprolifer-*
699 *ative neoplasms: Role and mechanisms of chronic inflammation*, Mediators of Inflam-
700 mation, (2015), pp. 1–16.
- 701 [28] T. HILLEN, H. ENDERLING, AND P. HAHNFELDT, *The Tumor Growth Paradox and*
702 *Immune System-Mediated Selection for Cancer Stem Cells*, Bulletin of Mathematical
703 Biology, 75 (2013), pp. 161–184.
- 704 [29] M. HULTCRANTZ, M. BJÖRKHOLM, P. W. DICKMAN, O. LANDGREN, A. R.
705 DEROLF, S. Y. KRISTINSSON, AND T. M. ANDERSSON, *Risk for Arterial and Ve-*
706 *nous Thrombosis in Patients With Myeloproliferative Neoplasms: A Population-Based*
707 *Cohort Study*, Annals of Internal Medicine, 168 (2018), pp. 317–325.

- 708 [30] J.-J. KILADJIAN, B. CASSINAT, S. CHEVRET, P. TURLURE, N. CAMBIER, M. ROUS-
709 SEL, S. BELLUCCI, B. GRANDCHAMP, C. CHOMIENNE, AND P. FENAUX, *Pegylated*
710 *interferon-alfa-2a induces complete hematologic and molecular responses with low tox-*
711 *icity in polycythemia vera*, *Blood*, 112 (2008), pp. 3065–3072.
- 712 [31] J.-J. KILADJIAN, S. GIRAUDIER, AND B. CASSINAT, *Interferon-alpha for the therapy*
713 *of myeloproliferative neoplasms: Targeting the malignant clone*, *Leukemia*, 30 (2016),
714 pp. 776–781.
- 715 [32] P. S. KIM, P. P. LEE, AND D. LEVY, *A PDE Model for Imatinib-Treated Chronic*
716 *Myelogenous Leukemia*, *Bulletin of Mathematical Biology*, 70 (2008), pp. 1994–2016.
- 717 [33] K. Y. KING AND M. A. GOODELL, *Inflammatory modulation of HSCs: viewing*
718 *the HSC as a foundation for the immune response*, *Nature Reviews Immunology*, 11
719 (2011-09-09), pp. 685–92.
- 720 [34] N. L. KOMAROVA, *Principles of Regulation of Self-Renewing Cell Lineages*, *PLoS*
721 *ONE*, 8 (2013), pp. 1–12.
- 722 [35] N. L. KOMAROVA, E. BARNES, P. KLENERMAN, AND D. WODARZ, *Boosting im-*
723 *munity by antiviral drug therapy: A simple relationship among timing, efficacy, and*
724 *success*, *Proceedings of the National Academy of Sciences*, 100 (2003), pp. 1855–1860.
- 725 [36] N. L. KOMAROVA AND D. WODARZ, *Effect of cellular quiescence on the success of*
726 *targeted CML therapy*, *PLoS ONE*, (2007).
- 727 [37] S. KOSCHMIEDER, T. MUGHAL, H. C. HASSELBALCH, G. BAROSI, P. VALENT, J.-J.
728 KILADJIAN, G. JERYCZYNSKI, H. GISSLINGER, J. JUTZI, J. PAHL, R. HEHLMANN,
729 A. VANNUCCHI, F. CERVANTES, R. SILVER, AND T. BARBUI, *Myeloproliferative neo-*
730 *plasms and inflammation: whether to target the malignant clone or the inflammatory*
731 *process or both*, *Leukemia*, 30(5) (2016), pp. 1018–24.
- 732 [38] H. LEE-SIX, N. F. ØBRO, M. S. SHEPHERD, S. GROSSMANN, K. DAWSON, M. BEL-
733 MONTE, R. J. OSBORNE, B. J. P. HUNTLY, I. MARTINCORENA, E. ANDERSON,
734 L. O’NEILL, M. R. STRATTON, E. LAURENTI, A. R. GREEN, D. G. KENT, AND
735 P. J. CAMPBELL, *Population dynamics of normal human blood inferred from somatic*
736 *mutations.*, *Nature*, 561 (2018-09-01), pp. 473,478.
- 737 [39] J. LEI AND M. C. MACKEY, *Multistability in an age-structured model of hematopoiesis*
738 *: Cyclical neutropenia*, *Journal of Theoretical Biology*, 270 (2011), pp. 143–153.
- 739 [40] I. R. LEMISCHKA, D. H. RAULET, AND R. C. MULLIGAN, *Developmental potential*
740 *and dynamic behavior of hematopoietic stem cells*, *Cell*, 45 (1986), pp. 917–927.

- 741 [41] A. LINDHOLM SØRENSEN AND H. C. HASSELBALCH, *Smoking and philadelphia-*
742 *negative chronic myeloproliferative neoplasms*, *European Journal of Haematology*, 97
743 (2016), pp. 63–69.
- 744 [42] P. LUNDBERG, A. KAROW, R. NIENHOLD, R. LOOSER, H. HAO-SHEN, I. NISSEN,
745 S. GIRSBERGER, T. LEHMANN, J. PASSWEG, M. STERN, C. BEISEL, R. KRALOVICS,
746 AND R. C. SKODA, *Clonal evolution and clinical correlates of somatic mutations in*
747 *myeloproliferative neoplasms.*, *Blood*, 123 (2014-04-03), pp. 2220,2228.
- 748 [43] M. C. MACKEY, *Cell kinetic status of haematopoietic stem cells*, *Cell Proliferation*,
749 34 (2001), pp. 71–83.
- 750 [44] A. L. MACLEAN, S. FILIPPI, AND M. P. H. STUMPF, *The ecology in the hematopoi-*
751 *etic stem cell niche determines the clinical outcome in chronic myeloid leukemia*, *Pro-*
752 *ceedings of the National Academy of Sciences*, 111 (2014), pp. 3883–3888.
- 753 [45] E. MANESSO, J. TELES, D. BRYDER, AND C. PETERSON, *Dynamical modelling of*
754 *haematopoiesis: an integrated view over the system in homeostasis and under per-*
755 *turbation.*, *Journal of the Royal Society, Interface / the Royal Society*, 10 (2013),
756 p. 20120817.
- 757 [46] A. MARCINIAK-CZOCRA, T. STIEHL, A. D. HO, W. JÄGER, AND W. WAGNER,
758 *Modeling of asymmetric cell division in hematopoietic stem cells—regulation of self-*
759 *renewal is essential for efficient repopulation.*, *Stem cells and development*, 18 (2009),
760 pp. 377–385.
- 761 [47] J. D. MEISS, *Differentiable Dynamical Systems*, SIAM, 1st ed., 2007.
- 762 [48] F. MICHOR, *Mathematical models of cancer stem cells*, *Journal of Clinical Oncology*,
763 26 (2008), pp. 2854–2861.
- 764 [49] F. MICHOR, T. P. HUGHES, Y. IWASA, S. BRANFORD, N. P. SHAH, C. L. SAWYERS,
765 AND M. A. NOWAK, *Dynamics of chronic myeloid leukaemia*, *Nature*, 435 (2005),
766 pp. 1267–1270.
- 767 [50] C. NIELSEN, H. S. BIRGENS, B. G. NORDESTGAARD, L. KJÆR, AND S. E. BO-
768 JESEN, *The JAK2 V617F somatic mutation, mortality and cancer risk in the general*
769 *population*, *Haematologica*, 96 (2011), pp. 450–453.
- 770 [51] J. T. OTTESEN, R. K. PEDERSEN, Z. SAJID, J. GUDMAND-HØYER, K. O. BANGS-
771 GAARD, V. SKOV, L. KJÆR, T. A. KNUDSEN, N. PALLISGAARD, H. C. HASSEL-
772 BALCH, AND M. ANDERSEN, *Bridging blood cancers and inflammation: The reduced*
773 *cancititis model*, *Journal of Theoretical Biology*, 465 (2019), pp. 90 – 108.

- 774 [52] J. PILLAY, I. DEN BRABER, N. VRISEKOO, L. M. KWAST, R. J. DE BOER, J. A. M.
775 BORGHANS, K. TESSELAAR, AND L. KOENDERMAN, *In vivo labeling with $2H_2O$ re-*
776 *veals a human neutrophil lifespan of 5.4 days*, *Blood*, 116 (2010), pp. 625–627.
- 777 [53] A. QUINTÁS-CARDAMA, O. ABDEL-WAHAB, T. MANSHOURI, O. KILPIVAARA,
778 J. CORTES, A.-L. ROUPIE, S.-J. ZHANG, D. HARRIS, Z. ESTROV, H. KANTARJIAN,
779 R. L. LEVINE, AND S. VERSTOVSEK, *Molecular analysis of patients with polycythemia*
780 *vera or essential thrombocythemia receiving pegylated interferon alpha-2a*, *Blood*, 122
781 (2013), pp. 893–901.
- 782 [54] S. RAO, *Stability analysis of the Michaelis - Menten approximation of a mixed mech-*
783 *anism of a phosphorylation system*, *Mathematical Biosciences*, 301 (2018), pp. 159 –
784 166.
- 785 [55] C. ROBINSON, *Dynamical systems, stability, symbolic dynamics, and chaos*, *Studies*
786 *in advanced mathematics*, CRC Press, Boca Raton, Fla, 2. ed. ed., 1999.
- 787 [56] I. A. RODRIGUEZ-BRENES, N. L. KOMAROVA, AND D. WODARZ, *Evolutionary dy-*
788 *namics of feedback escape and the development of stem-cell-driven cancers*, *Proceed-*
789 *ings of the National Academy of Sciences*, 108 (2011), pp. 18983–18988.
- 790 [57] I. ROEDER, M. HORN, GLAUCHE, A. HOCHHAUS, M. MUELLER, AND M. LOEFFLER,
791 *Dynamic modeling of imatinib treated chronic myeloid leukemia: functional insights*
792 *and clinical implications*, *Nature Medicine*, 12 (2006), pp. 1181–1184.
- 793 [58] S. RUBINOW AND J. LEBOWITZ, *A mathematical model of neutrophil production and*
794 *control in normal man*, *Journal of Mathematical Biology*, 1 (1975), pp. 187–225.
- 795 [59] Z. SAJID, M. ANDERSEN, AND J. T. OTTESEN, *Mathematical analysis of the can-*
796 *cinitis model and the role of inflammation in blood cancer progression*, *Mathematical*
797 *Biosciences and Engineering*, 16 (2019), pp. 8268–8289.
- 798 [60] J. L. SPIVAK, *The myeloproliferative neoplasms*, *New England Journal of Medicine*,
799 376 (2017), pp. 2168–81.
- 800 [61] T. STIEHL, N. BARAN, A. D. HO, AND A. MARCINIAK-CZOCHRA, *Cell Division*
801 *Patterns in Acute Myeloid Leukemia Stem-like Cells Determine Clinical Course: A*
802 *Model to Predict Patient Survival*, *Cancer Research*, 75 (2015), pp. 940–949.
- 803 [62] T. STIEHL, A. D. HO, AND A. MARCINIAK-CZOCHRA, *Mathematical modeling of*
804 *the impact of cytokine response of acute myeloid leukemia cells on patient prognosis*,
805 *Scientific Reports*, 8 (2018), pp. 1–11.
- 806 [63] T. STIEHL, C. LUTZ, AND A. MARCINIAK-CZOCHRA, *Emergence of heterogeneity in*
807 *acute leukemias*, *Biology Direct*, 11 (2016-10-12), p. 51.

- 808 [64] T. STIEHL AND A. MARCINIAK-CZUCHRA, *Characterization of stem cells using math-*
809 *ematical models of multistage cell lineages*, *Mathematical and Computer Modelling*,
810 53 (2011), pp. 1505 – 1517.
- 811 [65] T. STIEHL AND A. MARCINIAK-CZUCHRA, *Mathematical Modeling of Leukemogenesis*
812 *and Cancer Stem Cell Dynamics*, *Mathematical Modelling of Natural Phenomena*, 7
813 (2012), pp. 166–202.
- 814 [66] T. STIEHL, A. MARCINIAK-CZUCHRA, P. GREULICH, AND B. MACARTHUR, *Stem*
815 *cell self-renewal in regeneration and cancer: Insights from mathematical modeling*,
816 *Current Opinion in Systems Biology*, 5 (2017), pp. 112–120.
- 817 [67] A. TRAUlsen, J. M. PACHECO, L. LUZZATTO, AND D. DINGLI, *Somatic mutations*
818 *and the hierarchy of hematopoiesis*, *BioEssays*, 32 (2010), pp. 1003–1008.
- 819 [68] H. VAZIRI, W. DRAGOWSKA, R. C. ALLSOPP, T. E. THOMAS, C. B. HARLEY, AND
820 P. M. LANSDORP, *Evidence for a mitotic clock in human hematopoietic stem cells:*
821 *loss of telomeric DNA with age.*, *Proceedings of the National Academy of Sciences*,
822 91 (1994), pp. 9857–9860.
- 823 [69] E. VOIT, *A first course in system biology*, Garland Science, Taylor & Francis Group,
824 New York and London, 2013.
- 825 [70] P. R. WHEATER, *Functional histology: A text and colour atlas.*, Churchill Living-
826 stone., Edinburgh, 2nd. ed. ed., 1987.
- 827 [71] K. WILKIE, *Systems Biology of Tumor Dormancy. Chapter 10. A review of mathemat-*
828 *ical models of cancer-immune interactions in the context of tumor dormancy*, vol. 734,
829 Springer-Verlag, New York, 2013.
- 830 [72] D. WODARZ AND N. KOMAROVA, *Dynamics of cancer. Mathematical foundations of*
831 *oncology*, World Scientific Publishing, 2014.
- 832 [73] X. XU, Q. ZHANG, J. LUO, S. XING, Q. LI, S. B. KRANTZ, X. FU, AND Z. J.
833 ZHAO, *JAK2V617F: prevalence in a large Chinese hospital population*, *Blood*, 109
834 (2007), pp. 339–342.
- 835 [74] J. ZHANG, A. G. FLEISCHMAN, D. WODARZ, AND N. L. KOMAROVA, *Determining*
836 *the role of inflammation in the selection of JAK2 mutant cells in myeloproliferative*
837 *neoplasms*, *Journal of Theoretical Biology*, (2017).